

**ULTRATHIN TITANIUM DIOXIDE  
COATINGS ON CARBON NANOTUBES FOR  
STABLE LITHIUM OXYGEN BATTERY  
CATHODES**

A THESIS SUBMITTED TO  
THE GRADUATE SCHOOL OF ENGINEERING AND SCIENCE  
OF BILKENT UNIVERSITY  
IN PARTIAL FULFILLMENT OF THE REQUIREMENTS FOR  
THE DEGREE OF  
MASTER OF SCIENCE  
IN  
MATERIALS SCIENCE AND NANOTECHNOLOGY

By  
Faruk Okur  
October, 2016

ULTRATHIN TITANIUM DIOXIDE COATINGS ON CARBON  
NANOTUBES FOR STABLE LITHIUM OXYGEN BATTERY  
CATHODES

By Faruk Okur

October, 2016

We certify that we have read this thesis and that in our opinion it is fully adequate,  
in scope and in quality, as a thesis for the degree of Master of Science.

---

Eda Yılmaz(Advisor)

---

Burak Ülgüt

---

Hüsnü Emrah Ünalın

Approved for the Graduate School of Engineering and Science:

---

Ezhan Karışan  
Director of the Graduate School

## ABSTRACT

# ULTRATHIN TITANIUM DIOXIDE COATINGS ON CARBON NANOTUBES FOR STABLE LITHIUM OXYGEN BATTERY CATHODES

Faruk Okur

M.S. in Materials Science and Nanotechnology

Advisor: Eda Yılmaz

October, 2016

Fossil fuels hold the biggest share in energy sources for a very long time, especially in transportation, because of their appealing properties like very high energy efficiency, easy transport to any place in the world, very straightforward usage principle and they used to be quite abundant. However fossil fuel consumption results into release of harmful greenhouse gasses that causes global warming. On the other hand fossil fuels are not very abundant anymore and as a product that is formed in millions of years, the increasing energy demand worsens the situation. That is why renewable energy sources are more and more pronounced each day in the last half century. Nonetheless, irregular nature of the renewable energy sources makes them highly unpractical. Energy can only be harvested from renewable energy sources in specific time or specific locations, for instance, it is not possible to harvest energy from sun all day long or wind turbines can only be efficient in the places that there is sufficient wind power. This being the case, a clever approach is needed in order to be able to benefit from such convenient energy sources.

Energy storage systems are the saviour in this picture since they can be used to store the energy that is produced from renewable energy sources and available when needed. For instance, lithium oxygen (Li-O<sub>2</sub>) batteries are a very promising candidates for a replacement of fossil fuels in transportation due to their very high theoretical gravimetric energy density. Oxygen is used as active cathode material in Li-O<sub>2</sub> batteries, which enables them to have approximately ten times more battery capacity than state of art lithium ion batteries and ability to compete with fossil fuels. However there are some challenges to be addressed for Li-O<sub>2</sub> batteries to become a commercial technology. These challenges are mainly centered around

unwanted side product formations on cathode-electrolyte interface. These side products are accumulating on the cathode surface upon battery cycling and result into drastic capacity fading. Especially carbon based materials are not stable against battery cycling in Li-O<sub>2</sub> batteries even though they have quite profitable features as a cathode material for Li-O<sub>2</sub> batteries, such as; high surface area, low weight, high electrical conductivity, good oxygen reduction reaction activity etc.

In this thesis study, the motivation is to increase the stability of carbon nanotubes (CNTs) while benefiting from their aforementioned advantages in Li-O<sub>2</sub> batteries. In order to achieve this, an ultrathin and uniform titanium dioxide (TiO<sub>2</sub>) layer is coated on CNT surface by atomic layer deposition method. Prior to TiO<sub>2</sub> coating an effective functionalization method is introduced to CNT surfaces to facilitate a uniform coating. Transmission electron microscopy imaging and x-ray diffractometer analysis are performed to observe coating properties. X-ray photoelectron spectroscopy analysis and scanning electron microscopy imaging show the subsided side reactions, proving the stability of the TiO<sub>2</sub> coated CNT cathode. TiO<sub>2</sub> protective layer significantly prevents side product formation due to reduced cathode degradation and shows superior capacity retention compared to pristine CNT cathode upon full capacity battery cycling.

*Keywords:* Lithium-oxygen battery, Electrochemical energy storage, Non-carbon interface, Atomic layer deposition, TiO<sub>2</sub> coating, Multiwalled carbon nanotubes.

## ÖZET

# ULTRA İNCE TİTANYUM DİOKSİT KAPLI DAYANIKLI LİTYUM OKSİJEN PİLİ KATOTU

Faruk Okur

Malzeme Bilimi ve Nanoteknoloji, Yüksek Lisans

Tez Danışmanı: Eda Yılmaz

Ekim, 2016

Fosil yakıtlar, yüksek enerji verimleri, dünyanın her yerine kolayca taşınabilmeleri, oldukça standart kullanım prensipleri ve dünyada oldukça yaygın olmaları gibi çok sayıda önemli özelliklerinden dolayı uzun bir süredir, özellikle ulaşım sektöründe, enerji kaynakları arasında en büyük paya sahiplerdir. Ancak fosil yakıt tüketimi sera etkisi oluşturan zararlı gazların salınımına yol açtığı için küresel ısınmaya neden olmakla beraber rezervleri de tükenmektedir. Oluşması milyonlarca yıl süren bir ürün oldukları göz önünde bulundurulunca, giderek artan enerji talebi durumu daha da kötü bir hale sokmaktadır. Bu nedenden dolayı son yarım yüzyılda yenilenebilir enerji kaynaklarına olan ilgi her geçen gün artmaktadır. Buna rağmen yenilenebilir enerji kaynaklarının düzensiz yapısı onları oldukça kullanışsız bir seçenek haline getirmiştir. Enerji, yenilenebilir enerji kaynaklarından yalnızca belirli zamanlarda veya belirli mekanlardan elde edilebilir, örneğin, güneş enerjisinden bütün gün verim almak mümkün değildir ya da rüzgar türbinleri ancak yeterli rüzgar gücünün olduğu yerlerde verimli olur. Durum böyle olunca, bu değerli enerji kaynaklarından yararlanabilmek için akıllıca bir yaklaşıma ihtiyaç duyulmaktadır.

Yenilenebilir enerji kaynaklarından üretilen enerjiyi depolayıp gerektiğinde kullanımlarına olanak sağlayabilecek olan enerji depolama sistemleri, bahsedilen probleme mantıklı bir çözüm sunmaktadırlar. Teorik olarak oldukça yüksek enerji kapasitelerine sahip olan ve ulaşım sektöründe fosil yakıtlara alternatif olarak önemli bir gelecek vaat eden lityum oksijen ( $\text{Li-O}_2$ ) pilleri, enerji depolama sistemleri için iyi bir örnektir. Oksijen gazının aktif katot malzemesi olarak kullanılma özelliği  $\text{Li-O}_2$  pillerini, lityum iyon pillerine kıyasla yaklaşık olarak on kat daha fazla enerji kapasitesine ulaştırmış ve fosil yakıtlarla yarışabilir duruma getirmiştir. Buna rağmen  $\text{Li-O}_2$  pillerinin ticari bir teknoloji haline gelebilmesi için aşılması

gereken bazı problemler vardır. Bu problemler genel olarak katot ile elektrolit arayüzünde meydana gelen istenmeyen yan ürünlerin oluşumuyla alakalıdır. Bu yan ürünler katot yüzeyinde birikip katotun elektriksel iletkenliğini düşürerek pil çevrimleri süresince kapasiteyi büyük ölçüde düşürmektedirler. Özellikle karbon bazlı malzemeler, büyük yüzey alanı, düşük ağırlık, yüksek elektriksel iletkenlik ve iyi oksijen indirgenme reaksiyonu aktivitesi gibi Li-O<sub>2</sub> pil katotları için oldukça faydalı özellikler barındırmalarına rağmen, pil çevrimlerine karşı dayanıklı değildir.

Bu tez çalışmasının motivasyonu karbon nanotüplerin (CNT) Li-O<sub>2</sub> pillerinde dayanıklılığını arttırıp yukarıda bahsedilen faydalı özelliklerinden yararlanılabilir hale getirmektir. Bunu yapabilmek için CNT'lerin yüzeyi ultra ince ve düzenli bir titanyum dioksit (TiO<sub>2</sub>) tabakasıyla, atomik tabaka kaplama (ALD) metodu kullanarak kaplanmıştır. TiO<sub>2</sub> kaplanmadan önce, düzenli bir kaplama elde edebilmek için, CNT'lerin yüzeylerine etkili bir yüzey modifikasyonu işlemi uygulanmıştır. Kaplama özelliklerinin incelenmesi amacıyla geçirmeli elektron mikroskobu (TEM) ve X-ışını difraksiyonu (XRD) analizleri yapılmıştır. TiO<sub>2</sub> kaplı CNT katotlarının dayanıklılığını kanıtlayan, miktarı azalan yan ürünlerin incelenmesi için taramalı elektron mikroskobu (SEM) ve X-ışını fotoelektron spektroskopisi (XPS) analizleri yapılmıştır. TiO<sub>2</sub> koruyucu tabakası katot degradasyonunu azaltarak yan ürün oluşumunu büyük ölçüde engellemiş ve saf CNT katotuyla karşılaştırıldığında tam kapasite pil çevrimlerinde üstün bir kapasite korunumu göstermiştir.

*Anahtar sözcükler:* Lityum-oksijen pili, Elektrokimyasal enerji depolama, karbonsuz arayüz, Atomic layer deposition, TiO<sub>2</sub> kaplama, çoklu duvarlı karbon nanotüpleri.

## Acknowledgement

It is a great pleasure for me to acknowledge my academic advisor, Dr. Eda Yılmaz, for her support and guidance throughout my dissertation. She provided me and other EESL group members a beneficial, professional, understanding and welcoming work environment with lots of valuable knowledge and experiences. I would like to acknowledge my thesis collaborator Dr. Necmi Bıyıklı and also Hamit Eren for their valuable contribution to this thesis work.

It was a pleasure to work and exchange ideas with all EESL group members; Mehmet Can Yağcı, Kıvanç Çoban, Ömer Ulaş Kudu, Mohammed Fathi Tovini, Dr. Cevriye Koz and Dr. Bhushan Patil. I would like to thank them all for their help, support, valuable advises and especially for their friendship. I would also like to thank my friends Mustafa Fadlelmula, Sağnak Sağkal, Hatice Kübra Kara, Ababakar Isa Adamu, Fatih Yergöz, İdil Uyan, Nurcan Haştar, Merve Şen and many others in UNAM for being there.

I would especially like to thank my family for their invaluable support. I hereby specially dedicate this thesis to my fiancée, Zeynep and thank her for her support, company, encouragement and love that have given me strength and self-confidence during hard times.

Finally, I would like to acknowledge TUBITAK, for funding, 114M478 and 214M437 numbered projects.

# Contents

<b>1</b>	<b>Introduction</b>	<b>1</b>
1.1	Energy Storage . . . . .	1
1.1.1	Electrochemical Energy Storage . . . . .	3
1.2	Batteries . . . . .	3
1.2.1	Lithium Batteries . . . . .	7
1.3	Li-O <sub>2</sub> Batteries . . . . .	11
1.4	Motivation . . . . .	17
<b>2</b>	<b>Materials and Methods</b>	<b>19</b>
2.1	Materials . . . . .	19
2.1.1	Cathode and Electrolyte Preparation . . . . .	19
2.1.2	Li-O <sub>2</sub> Battery Cell Configuration . . . . .	21
2.2	Characterization . . . . .	22
2.3	Electrochemical Tests . . . . .	24

<b>3 Results and Discussion</b>	<b>26</b>
3.1 CNT Surface Modification . . . . .	28
3.1.1 Plasma Ashing . . . . .	28
3.1.2 CTAB Surface Modification . . . . .	33
3.1.3 Acid Functionalization . . . . .	37
3.2 Optimization of TiO <sub>2</sub> Coating . . . . .	39
3.3 Stability Tests of Li-O <sub>2</sub> Battery Cathode . . . . .	47
<b>4 Conclusions</b>	<b>57</b>

# List of Figures

1.1	World energy consumption, 1990-2040 (quadrillion Btu) (OECD: Countries inside the Organization for Economic Cooperation and Development), b) World net electricity generation by energy source, 2010-2040 (trillion kilowatthours). . . . .	2
1.2	Specific power against specific energy, also called a ragone plot, for various electrical energy storage devices. If a supercapacitor is used in an electric vehicle, the specific power shows how fast one can go, and the specific energy shows how far one can go on a single charge. Times shown are the time constants of the devices, obtained by dividing the energy density by the power. . . . .	4
1.3	Battery chemistry over the years. Present-day battery technologies are being outpaced by the ever- increasing power demands from new applications. As well as being inherently safe, batteries of the future will have to integrate the concept of environmental sustainability. . . . .	5
1.4	Graph of mass and volume energy densities of several secondary cells (by direction: down=heavier, up=lighter, right=powerful, left=weaker). . . . .	8
1.5	A schematic representation of the working mechanism of a simple LIB. . . . .	10

1.6	The gravimetric energy densities ( $\text{Whkg}^{-1}$ ) for various types of rechargeable batteries compared to gasoline. The theoretical density is based strictly on thermodynamics and is shown as the blue bars while the practical achievable density is indicated by the orange bars and numerical values. For Li-air, the practical value is just an estimate. For gasoline, the practical value includes the average tank-to-wheel efficiency of cars. . . . .	12
1.7	A schematic representation of an aprotic Li-O <sub>2</sub> battery. . . . .	14
1.8	A schematic representation of one ALD cycle. . . . .	17
2.1	Schematic representation of Li-O <sub>2</sub> battery cell configuration. . . . .	22
2.2	XRD sample preparation scheme for analyzing the crystallization of TiO <sub>2</sub> after annealing. . . . .	23
2.3	Landt CT2001 multichannel potentiostat/galvanostat. . . . .	24
3.1	a) TEM Images of P-100T cathodes. White bars indicate 5 nm in scale, b) Battery performance of P-100T cathode at 100 $\text{mA}\text{g}^{-1}$ current rate. . . . .	29
3.2	TEM Images of P-25T cathodes. White bar indicate 5 nm and black indicate 2 nm in scale respectively. . . . .	30
3.3	TEM Images of P-50T cathodes. Black bar indicate 2 nm and dashed bar indicate 10 nm in scale respectively. . . . .	31
3.4	Battery performance comparison of P-100T, P-50T and P-25T cathodes at 100 $\text{mA}\text{g}^{-1}$ current rate. . . . .	31

3.5	TEM images of P-75T cathodes at a) 1,5 and b) 2 minutes of plasma ashing. Dashed and white bars represent 10 and 5 nm respectively. . . . .	32
3.6	TEM images of a) C-25, d) C-100 and Dark field TEM images of b) C-50 and c) C-75 cathodes. Black, dashed and white bars indicate 10, 50 and 20 nm in scale, respectively. . . . .	34
3.7	Battery performance comparison of C-25, C-50, C-75, C-100 and bare CNT cathodes. . . . .	35
3.8	TEM images of various cathodes before and after annealing: a) C-50T, b) C-50T-Ann, c) C-100T, d) C-100T-Ann, e) P-100T, f) P-100T-Ann. Dashed, black and white bars indicate 10, 5 and 2 nm in scale respectively. . . . .	36
3.9	TEM images of a) C-50T-Ann and b) C-100T-Ann cathodes. White bars indicate 10 nm in scale. . . . .	36
3.10	TEM images of sheet like layers in between CNTs of a) C-50T and b) C-100T cathodes. Black bars indicate 20 nm in scale. . . . .	37
3.11	a) TEM images of A-100T cathode. Black and dashed bars indicate 5 and 10 nm in scale, respectively. b) Battery cycling performance of A-100T cathode at $100 \text{ mA g}^{-1}$ current rate. . . . .	38
3.12	TEM images of a) A-50T, b) A-30T and c) A-20T cathodes. White bars indicate 5 nm in scale. . . . .	39
3.13	Discharge capacity retention comparison of A-50T, A-30T and A-20T cathodes on full 20 discharge and charge battery cycles at $100 \text{ mA g}^{-1}$ current rate. . . . .	40

3.14 XRD pattern of $\text{TiO}_2$ coated CNTs before and after annealing. CNT- $\text{TiO}_2$ Annealed pattern perfectly matches with Anatase phase $\text{TiO}_2$ (JCPDS file 21-1272). The peaks that are marked with asterisk are originating from Si-wafer, which the analyzed samples are casted on. . . . .	41
3.15 TEM images of a) A-50T-Ann, b) A-30T-Ann and c) A-20T-Ann cathodes. Black and white bars indicate 10 and 5 nm in scale, respectively. . . . .	42
3.16 Discharge capacity retention comparison of A-50T-Ann, A-30T-Ann and A-20T-Ann cathodes on full 20 discharge and charge battery cycles at $100 \text{ mAg}^{-1}$ current rate. . . . .	43
3.17 TEM images of a) A-10T-Ann, b) A-5T-Ann, c) A-1T-Ann and d) Acid functionalized CNT. Black and white bars indicate 2 and 5 nm in scale, respectively. . . . .	44
3.18 Discharge capacity retention comparison of A-10T-Ann, A-5T-Ann, A-1T-Ann and A-CNT cathodes on full 20 discharge and charge battery cycles at $100 \text{ mAg}^{-1}$ current rate. . . . .	45
3.19 Discharge capacity retention comparison of A-1T-Ann and CNT cathodes on full 20 discharge and charge battery cycles at $100 \text{ mAg}^{-1}$ current rate. . . . .	46
3.20 CV curves of a) CNT, b) 5T electrodes . . . . .	48
3.21 Full capacity discharge and charge curves of a) CNT, b) A-5T-Ann cathodes. . . . .	50

3.22	Nyquist plots of the impedance measurements before and after CV measurements of a) CNT, b) A-5T-Ann electrodes. OCV values for CNT electrode before and after CV are 2.786 V and 3.364 V respectively and for A-5T-Ann electrode before and after CV are 3.116 V and 3.393 V respectively. . . . .	52
3.23	a) C1s and b) O1s XPS spectra of CNT and A-5T-Ann cathodes in their pristine state and after cycling at the end of 20 <sup>th</sup> charge. . . . .	54
3.24	Li1s XPS spectra of CNT and A-5T-Ann cathodes after full capacity battery cycling at the end of 20 <sup>th</sup> charge. . . . .	55
3.25	SEM images of a, b) A-5T-Ann and c, d) CNT cathodes in their a, c) pristine state and b, d) after cycling at the end of 20 <sup>th</sup> charge. . . . .	56

# Chapter 1

## Introduction

### 1.1 Energy Storage

Energy need is one of the biggest issue in the world. With the rapidly developing technology, industrialization and increasing population, energy demand is now in its highest level in history and as a certainty, it will continue to increase. In fact, it has been reported that world energy consumption will grow by 56% between 2010 and 2040. (Figure 1.1a) There are many different sources of energy in the world and almost 80% of the energy is generated by fossil fuels, which is not likely to change too much considering the current state. (Figure 1.1) [1] Fossil fuels (e.g., oil, coal, petroleum, and natural gas) are comparatively the most efficient energy source up to date considering their many appealing features like high energy output, easy transport to any place in the world, very straightforward usage principle etc. which is the main reason why it is the mostly used source so far. However they have many downsides that push people to search for renewable energy sources in the last half century. First of all, fossil fuels are limited sources. Considering the global energy consumption, depletion of fossil fuels is not very far in the future. Related to this problem the fuel prices are rising up each day and this cause huge discomfort on intergovernmental relations. Apart from these issues, the most well-known and dangerous disadvantage of fossil fuels is

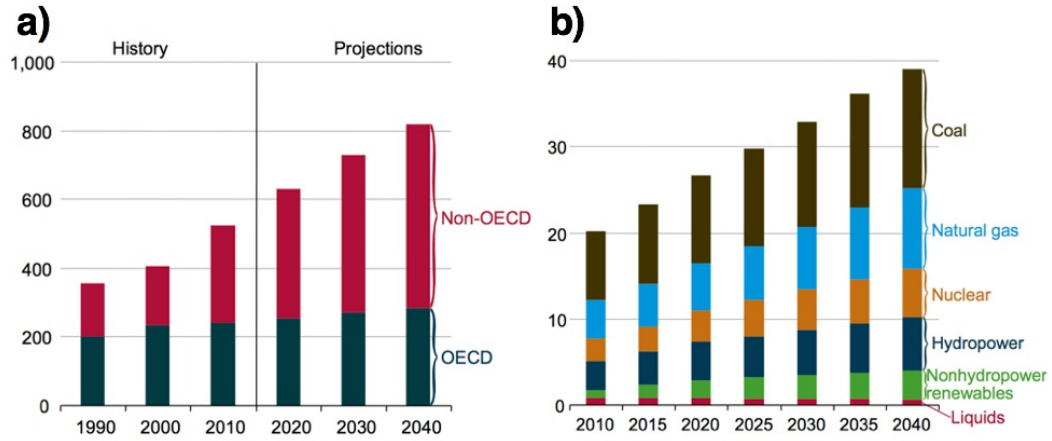


Figure 1.1: a) World energy consumption, 1990-2040 (quadrillion Btu) (OECD: countries inside the Organization for Economic Cooperation and Development), b) World net electricity generation by energy source, 2010-2040 (trillion kilowatt-hours). [1]

harmful greenhouse gas emissions on energy generation. It has been reported that fossil fuels own the biggest share on CO<sub>2</sub> emission in the world which cause global warming. [2,3] In order to reduce greenhouse gas emissions many countries adopting certain regulations but only this is not enough.

Considering the problematic features of fossil fuels, renewable energy sources should be shown the utmost importance. These renewable energy sources include solar, tidal, wind, hydro, biomass, and geothermal energies etc. Even though they are environmentally friendly, cheaper and limitless in source, they have their own limitations. Unfortunately these renewable energy sources are highly irregular. They are either not available throughout a day or dependant to specific regions which constrains a global usage. Exactly here, importance of energy storage comes into play. In order to be able to benefit from renewable energy sources, the generated energy need to be stored. Energy storage is basically converting an energy from that is difficult or non-conventional to store to a conventional form. There are many different types of energy storage such as mechanical, thermal, electrical, electrochemical etc. Electrochemical energy storage systems are the most proper energy storage systems to be used in electric vehicles considering their mobility, considerably good energy density and good energy output.

### 1.1.1 Electrochemical Energy Storage

Electrochemical energy storage is basically converting electrical energy to chemical energy and *vice versa*, if not primary cell, (throughout the text secondary or rechargeable cells will be discussed) by means of electrochemical redox reactions. Electrochemical energy storage devices can be divided into two categories; supercapacitors and batteries. They both consist of three main components; electrically conductive anode and cathode separated by an electrically insulator but ionically conductive electrolyte. Supercapacitors or electric double layer capacitors are electrochemical energy storage devices that supply high power in a short time. They have higher capacity than regular capacitors in other words they are in between capacitors and batteries and additionally they have much higher specific power density than both. [4,5] Supercapacitors are being used in applications that require high power in a short time such as; back-up systems for power suppliers, consumer electronics etc. [6] Recently supercapacitors even started to be used in emergency doors of Airbus A380, which shows their good performance and reliability. [7] Even though supercapacitors have those mentioned important applications, they are not suitable energy storage systems for electric vehicles. As can be seen from Figure 1.2, batteries are more suitable energy storage systems for electric vehicles because they enable long term energy supply, considering their specific capacity, durability and rather long cycle life.

## 1.2 Batteries

Batteries are electrochemical energy storage units that store energy electrochemically when connected to a power supply and deliver the energy to an external electric device when needed, repeatedly. Batteries store and produce energy by reversible electrochemical reactions. There are many battery types that are being used in our daily life for years. Generally batteries are very portable and practical energy storage systems, which considerably ease the usage on mobile devices.

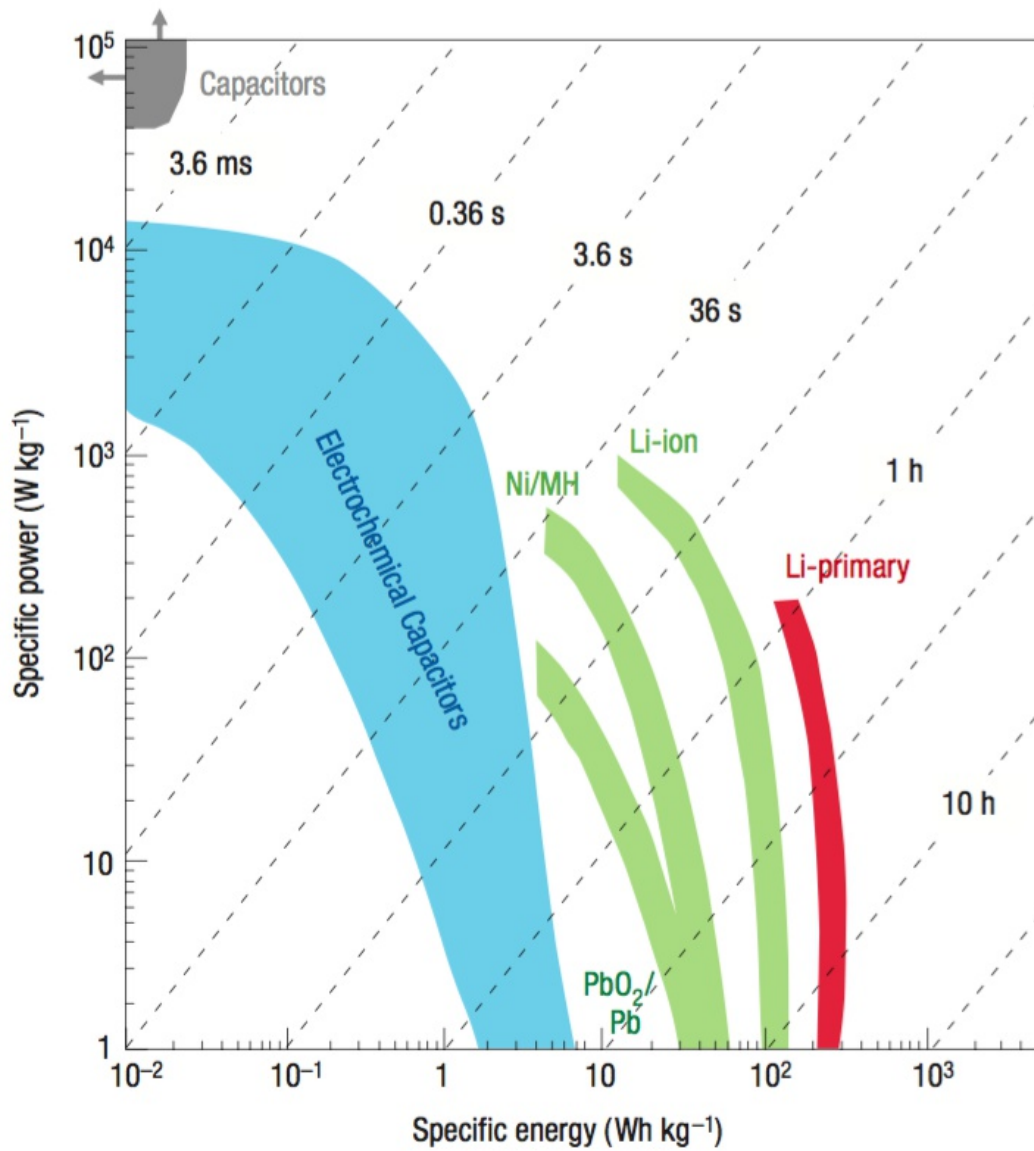


Figure 1.2: Specific power against specific energy, also called a ragone plot, for various electrical energy storage devices. If a supercapacitor is used in an electric vehicle, the specific power shows how fast one can go, and the specific energy shows how far one can go on a single charge. Times shown are the time constants of the devices, obtained by dividing the energy density by the power. [8]

The history of batteries goes up to early 1800s to the first discovery of electrochemical battery by Alessandro Volta. The first battery consisted of zinc and copper metals separated by brine-soaked paper disks, which supplied reasonable amount of current for a certain time. [9] In 1836, British chemist John Frederic Daniell upgrade Volta's invention and produced the first industrially usable battery which was used in electrical telegraphs by then. [10] Since those early years up to now, batteries have been developed quite a lot and today there are countless of consumer products that are working with different types of batteries.

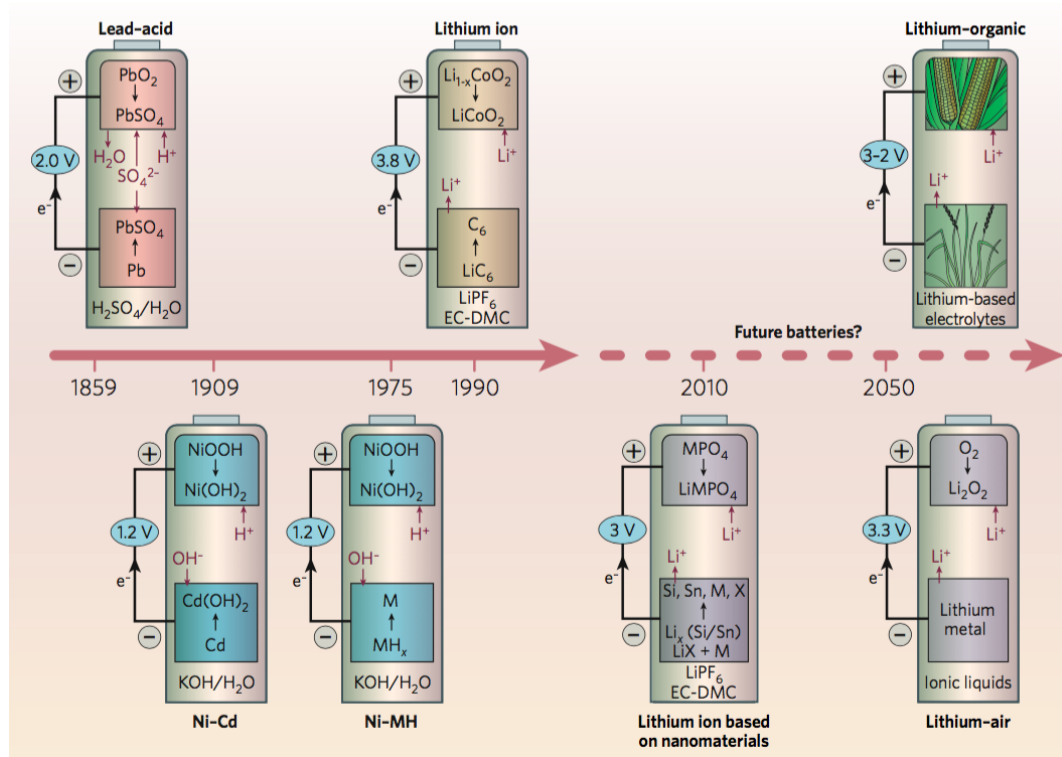


Figure 1.3: Battery chemistry over the years. Present-day battery technologies are being outpaced by the ever- increasing power demands from new applications. As well as being inherently safe, batteries of the future will have to integrate the concept of environmental sustainability. [11]

Batteries consist of three main parts as the other electrochemical energy storage systems; one negative electrode such as lithium, zinc etc., one positive electrode such as lithium cobalt oxide, manganese dioxide etc. and one electrically insulating but ionically conductive electrolyte. Anode and cathode materials are

chosen based on their electrical conductivity, stability in electrochemical environment and low cost alongside with their electrochemical activity. Electrolytes might be molten salts, dissociated salts in water or solvent solution and solid electrolytes. These three components of the batteries are the main determining factors of capacity, stability and also working mechanism of the batteries. For instance, in order to have a high energy storage capacity, it is wiser to choose higher chemical potential difference between the two electrodes.

The gravimetric energy density is based on potential difference between anodic and cathodic half reactions and also amount of charge stored per unit weight of materials. Electrolytes on the other hand play a critical role on electrochemical reactions and the stability of the batteries. In conjunction with these, electrode electrolyte interface is another important feature of the batteries since all the redox reactions happening in this region.

On discharge, the anode of the battery is oxidized, which means ions transport from anion to cation through electrolyte and meanwhile anode give electrons to outer circuit and supply energy to the connected device. On charge the exact opposite electrochemical reactions occur. In this case, a reverse voltage that is larger than the battery voltage is need to be given to the system in order for charging to happen.

There are a large number of battery types available in the market that are used for many different applications. Lead-acid batteries, lithium-ion batteries, nickel-metal hydride batteries, magnesium-ion batteries, vanadium-redox batteries and recently popular and promising lithium and sodium air (oxygen) batteries are just some of the examples. There are also many primary batteries that are not mentioned here. Some of the significantly important batteries will be briefly explained below and than lithium oxygen batteries will be discussed in details in a separate section.

Lead-acid batteries are the oldest rechargeable (secondary) batteries, which invented by French physicist Gaston Planté. Even though these batteries are very old and have a very low energy-to-weight and a low energy-to-volume ratio, they

are still frequently used in automobiles as motor starters thanks to their ability to supply high power-to-weight ratio and most importantly their low cost. [12] In fact, lead-acid batteries have a market value of \$15 billion at manufacturers levels and their sales account for approximately 40 to 45% of the sales of all batteries. [13]

Nickel-metal hydride (NIMH) batteries are another battery type that are frequently used in daily life in consumer electronics. In these batteries a hydrogen absorbing negative electrode is used. Because of their relatively high energy density and sealed construction, they are frequently used in cellular phones and other portable consumer products as a replacement of nickel-cadmium batteries. They are also more environmentally friendly than nickel-cadmium batteries considering cadmium free structure. In addition to these, larger sizes of NIMH batteries are even considered to be used in electric vehicles in some studies. [13,14]

### **1.2.1 Lithium Batteries**

Lithium is a very advantageous metal to be used in batteries as an anode material based on the fact that it is the most electropositive (3.04 V versus standard hydrogen electrode), a good electrically conductive as well as the lightest metal. [15] Because of these remarkable features, lithium metal has been used in primary and secondary batteries for a long time. Lithium based batteries hold 63% of worldwide sales value in portable batteries, which is the sign of their suitability. [16] In Figure 1.4, it can be seen that lithium based batteries are much better than other types of batteries in terms of energy density.

Using lithium metal in batteries was a progressive process. In 1970s, the electrochemical intercalation is realized [17], although it was not a general knowledge and only mentioned in a conference. In 1972, Exxon proposed  $\text{TiS}_2$  as a lithium intercalation material, which was approved by many scientist at that time. [18] Soon after they faced dendrite problem of lithium metal in the batteries. Dendrite formation is uneven lithium growth inside the batteries which can cause shortcircuits and finally combustion or even explosion. It is also called thermal runaway. [19]

This problem tried to be solved by alloying the lithium metal but this time they faced limited cyclability problem. Meanwhile in Bell Labs, there had been significant improvements on intercalation materials. [20] Finally in 1980s Goodenough introduced families of intercalation compounds that are still used almost exclusively in today's batteries. [21, 22] However at that time safety of lithium based batteries was still an issue. In order to overcome this problem exchanging metallic lithium with an insertion material was considered, that way lithium in ionic form would not cause dendrite problem. [23] Finally in 1991, a carbon based, highly reversible, low voltage, lithium intercalation - deintercalation material was discovered by Sony Corporation [24], which was the first utilization of Lithium ion batteries (LIBs). The discovered material was  $\text{Li}_x\text{C}_6/\text{Li}_{1-x}\text{CoO}_2$  and the battery cell is called rocking chair. [25] Back then LIB was storing energy around  $180 \text{ Whkg}^{-1}$  which was 5 times higher than current batteries at that time. [11]

Among the rechargeable batteries the most well known ones are LIBs. LIBs are commonly used in almost every portable everyday devices such as laptops, mobile phones, digital cameras, cordless drills, saws and so on, thanks to their low weight and high energy density. They are also considered to be used in cars as a replacement of lead-acid batteries and even in electric vehicles.

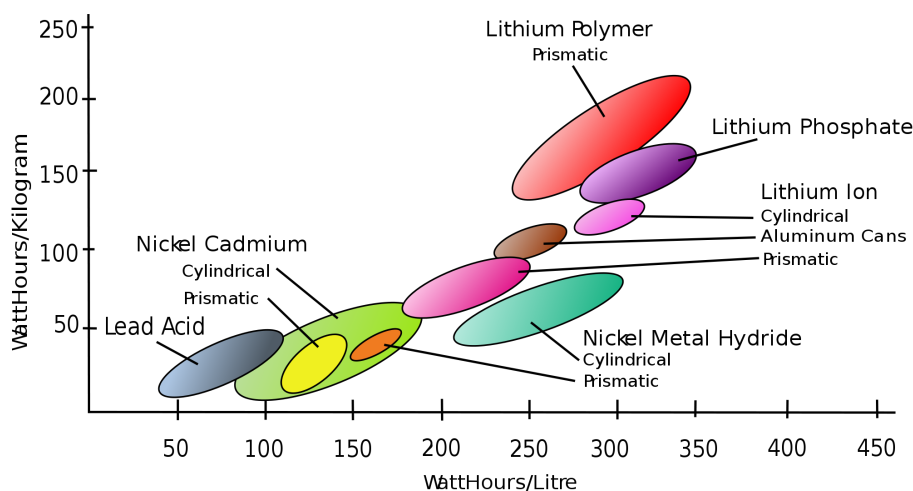
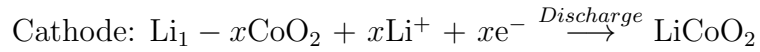
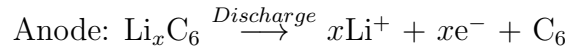


Figure 1.4: Graph of mass and volume energy densities of several secondary cells (by direction: down=heavier, up=lighter, right=powerful, left=weaker). [26]

The working mechanism of LIBs is basically intercalation and deintercalation of

lithium ions between two electrodes. On charge, lithium ions move from cathode to anode and intercalate inside the cathode structure and on discharge the ions are removed from anode back to cathode while generating electricity. In between two electrodes there is an electrolyte material that is electrically insulating and ionically conductive. The electrolyte can be liquid, solid or gel like material while liquid phase materials are commonly used which consist of a lithium salt such as;  $\text{LiPF}_6$ ,  $\text{LiBF}_4$ ,  $\text{LiClO}_4$  to enable  $\text{Li}^+$  conductivity that dissolves in a mixture of organic alkyl carbonate solvents like ethylene, dimethyl or diethyl. The energy storage in the "rocking chair" LIB is demonstrated in the following reactions: [27]



$$E = 3.7 \text{ V at } 25^\circ\text{C}$$

LIBs have several advantages over the other secondary battery types which made it the battery of choice for many devices in a few years. LIBs have high cell voltage levels up to 3.7 V. This means that one LIB accounts for approximately 3 NiCd or NiMH batteries. The other advantage is their already mentioned high gravimetric energy density and maybe the most fascinating one is their very high efficiency, which can be as high as 98% and they can reach very high number of battery cycles ranging between short and long period of times. [29]

Since its discovery there have been extensive studies to improve the characteristics of LIBs in terms of high capacity, stability and longer cycle life. However there has not been a complementary change in LIB chemistry since its introduction to the battery market. Most LIB still relies on graphite anode and lithium cobalt oxide cathode separated by an electrolyte. [30] Early stage LIBs were inherently unsafe because of unstable electrode and electrolyte materials in operating voltages. Certainly state of art LIBs are safer and suitable to use in many

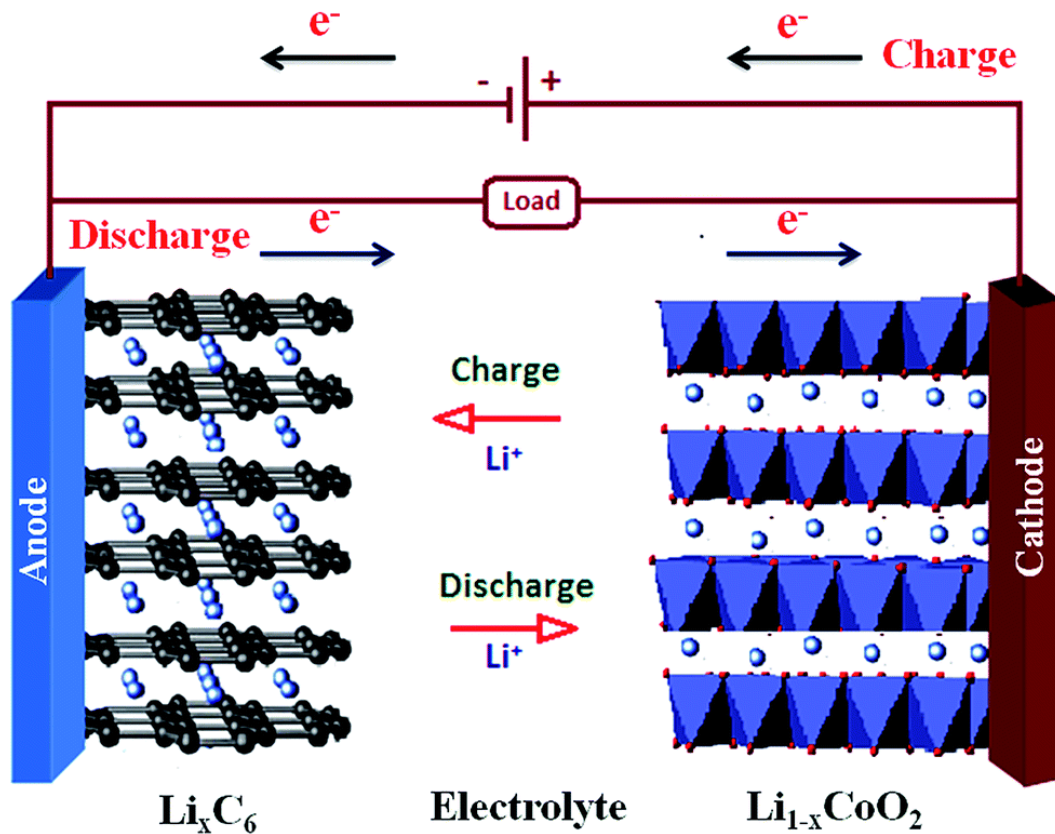


Figure 1.5: A schematic representation of the working mechanism of a simple LIB. [28]

electronic devices but scaling up still is an issue since such problems are more pronounced.

The performance and the efficiency of LIBs are limited with the properties of the materials that are being used in the batteries. That is why researches nowadays concentrated on the replacement of current battery components with more efficient ones. One of the most promising candidate for LIB anode material is silicon (Si). There are a lot of studies going on about using Si anodes in LIBs recently, because of its extremely high specific capacity. [31–33] However there is a major challenge that have to be addressed for this anode material, which makes it unstable in battery operations, that is large volume expansion and contraction through battery cycles. There are other promising anode materials for LIBs as well like lithium titanium oxide, lithium tin, lithium iron phosphate, several other metal oxides and micro and nano-structures. Even though LIBs

are well-established electrochemical energy storage systems for many portable devices and further improvements are possible with the extensive studies in the near future, they are not suitable for high capacity applications like electric vehicles. Being dependant on insertion mechanism, LIBs are strictly limited to one electron transfer per transition metal in terms of specific energy. In this case, in order to reach higher specific energies, fundamental changes are required in the electrochemical energy storage mechanism. Electrochemical conversion chemistry instead of insertion is considered as a reasonable choice. Metal-air batteries are in that sense, a considerable candidate for high energy density requiring energy storage systems thanks to their high specific capacities. Lithium-air or lithium oxygen (Li-O<sub>2</sub>) batteries are the most promising metal-air battery systems considering the already mentioned advantages of using lithium in a battery. In the following section Li-O<sub>2</sub> batteries, their promising features and challenges will be discussed.

### 1.3 Li-O<sub>2</sub> Batteries

Lithium air (Li-air) battery is a metal air battery type that composed of a lithium metal anode, porous and high surface area air cathode and a lithium ion conductive electrolyte material. Since in the future, the oxygen is proposed to be used directly from air as an active cathode material, they frequently called Li-air batteries. However the current technology is still in laboratory scale and pure oxygen gas is used in these batteries to avoid unwanted parasitic reactions with components, such as water, carbon dioxide, carbon monoxide, and nitrogen, in ambient air. The oxygen is generally supplied from an oxygen tank to the Li-air batteries. That is why most of the time lithium oxygen (Li-O<sub>2</sub>) is preferred to be used instead of Li-air. In order to realize a real Li-air battery cell a well-established oxygen diffusion membrane need to be produced. In fact there are a number of promising studies considering this issue. [34, 35]

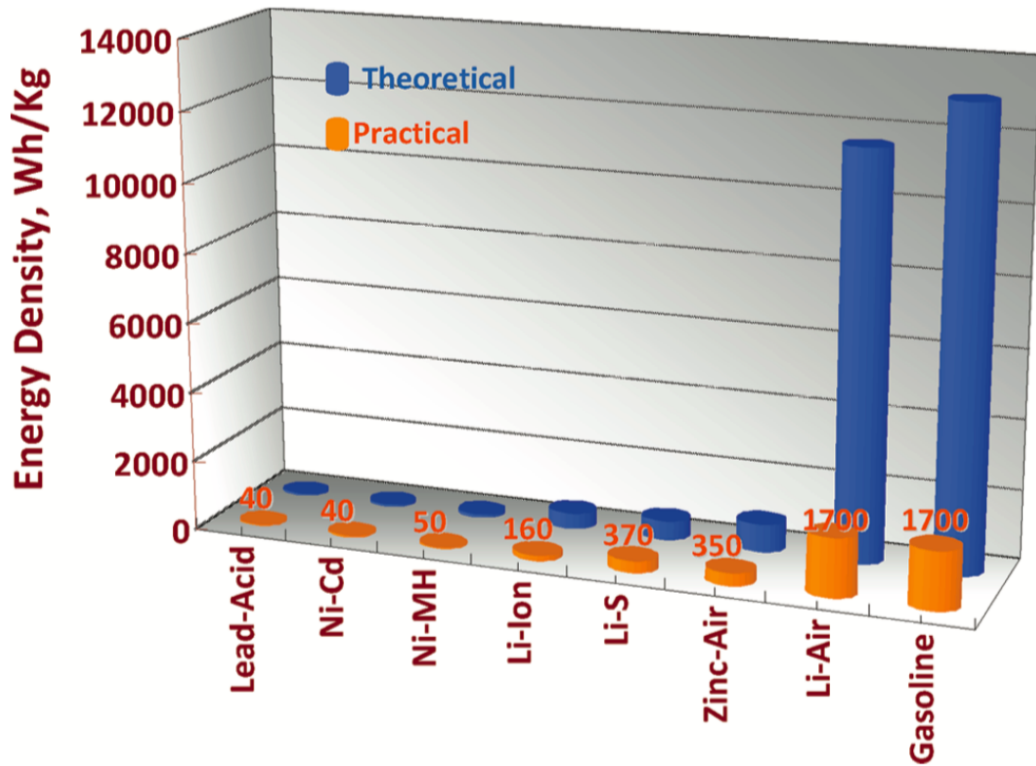


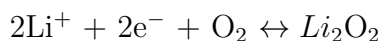
Figure 1.6: The gravimetric energy densities ( $\text{Whkg}^{-1}$ ) for various types of rechargeable batteries compared to gasoline. The theoretical density is based strictly on thermodynamics and is shown as the blue bars while the practical achievable density is indicated by the orange bars and numerical values. For Li-air, the practical value is just an estimate. For gasoline, the practical value includes the average tank-to-wheel efficiency of cars. [36]

Li-air batteries are first proposed by the researchers, Littauer and Tsai, at Lockheed Missiles and Space Company in 1976. [37] At that time the negative electrode lithium metal and the positive air electrode were unstable and risky to be used in batteries so Li-air batteries did not attract attention from market. Nevertheless, in 1990s, Li-air batteries started to attract interest due to the lack of a convenient energy storage system for electric vehicles and due to a promising study by Abraham and Jiang [38], which is the first study that proves the rechargeability of Li-air batteries, even though the risks of the electrodes pretty much were still there. Since that time, the studies about Li-air batteries grew exponentially and there have been many publications and patents concerning these batteries.

Li-O<sub>2</sub> batteries have been attracting attention especially in the past decade due to their promising attributes as an electrochemical energy storage system. Rechargeable Li-O<sub>2</sub> batteries have theoretical specific energy around 3500 Whkg<sup>-1</sup> which is almost 10 times more than LIBs, so they are expected to be a prospective alternative to gasoline in vehicles for transportation. [39] The exceptional theoretical energy density is coming from the weight advantage of the active cathode, oxygen, and extensive reaction sites for discharge products to form compared to intercalation limited capacity of Li-ion batteries. As can be seen from Figure 1.6, theoretical and practical gravimetric energy density of Li-air batteries are very close to that of gasoline.

There are four types of chemical architectures of Li-O<sub>2</sub> batteries in terms of electrolytes: aprotic, aqueous, mixed-electrolyte and fully solid-state batteries. The essential electrochemical reactions are very much dependant on the electrolyte configuration. Although all electrolyte types have their own advantages and disadvantages, aprotic electrolyte is mostly the preferred one in Li-O<sub>2</sub> battery studies in order to have a straightforward discharge product formation by avoiding complicated reactions with water and to have a good ionic conductivity compared to all solid state electrolyte batteries. Throughout this thesis work, Li-O<sub>2</sub> batteries with aprotic (non-aqueous) type electrolyte will be discussed.

In non-aqueous Li-O<sub>2</sub> batteries, the suggested net electrochemical reaction, developing on the cathode surface can be described as;



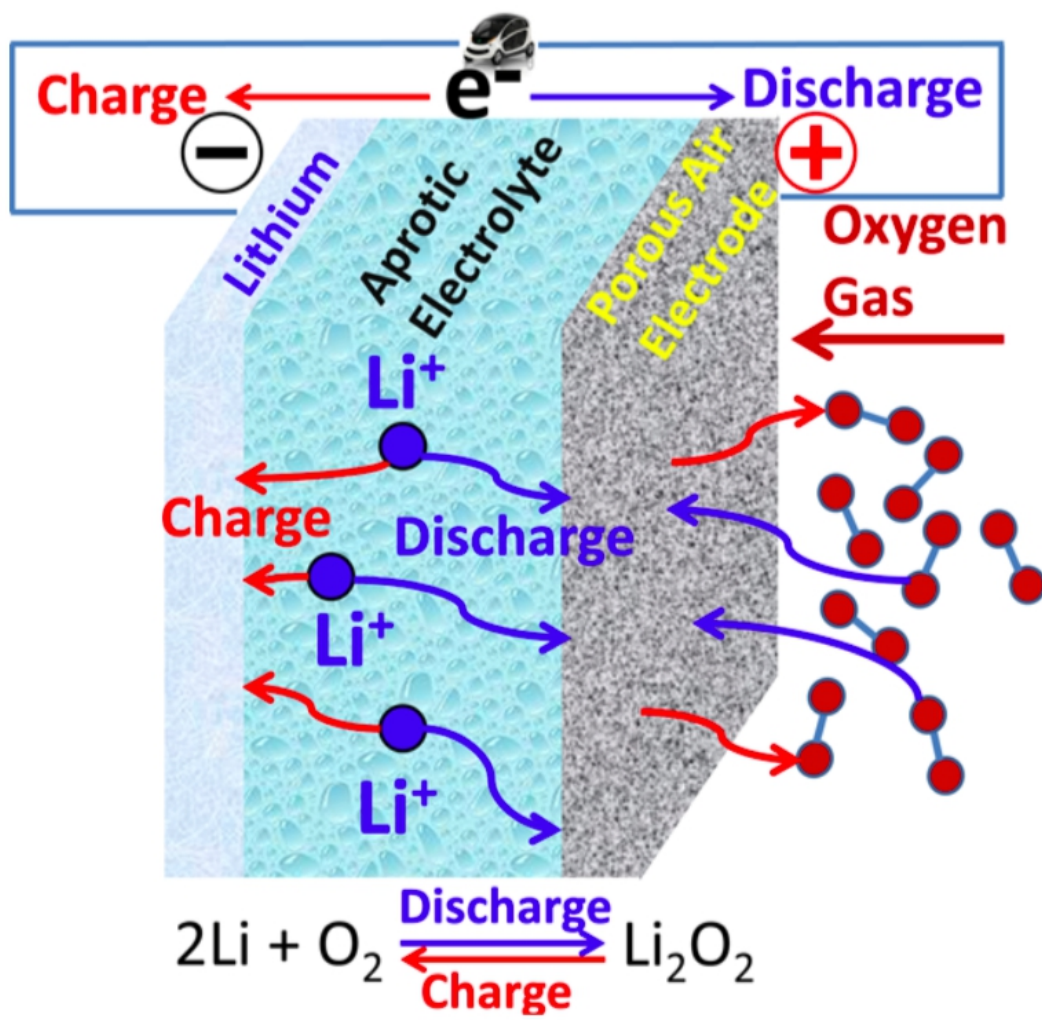


Figure 1.7: A schematic representation of an aprotic Li-O<sub>2</sub> battery. [40]

On discharge,  $\text{Li}^+$  ions combine with  $\text{O}_2$  molecules to form  $\text{Li}_2\text{O}_2$ , which is the main discharge product of  $\text{Li-O}_2$  batteries that accumulates on the cathode surface. Contrarily on charge,  $\text{Li}_2\text{O}_2$  on cathode surface disintegrate to  $\text{Li}^+$  ions and  $\text{O}_2$  molecules.

Despite having very promising attributes, there are some challenges to be addressed for  $\text{Li-O}_2$  batteries to become a commercial technology. [41] While many factors affect the  $\text{Li-O}_2$  battery performance such as humidity, [42] oxygen partial pressure, [43] macro-structure of the cathode, [44] and the overall cell design, [45] the crucial show-stopper problems related to this system are mainly centered around unwanted side product formations, caused from cathode and electrolyte degradation during cell operation. These side products accumulate on the cathode surface on subsequent cycles and reduce the electrical conductivity, which finally leads to capacity fading and cause limited cycling behavior. [41] In this regard, developing a stable cathode and electrolyte must be the main focus of  $\text{Li-O}_2$  battery studies to build up a high-performance battery system.

In  $\text{Li-O}_2$  batteries, the cathode material should fulfill some general requirements such as; high surface area, high pore volume, good electrical conductivity, and a structure to support fast gas transport. [46] In most of the  $\text{Li-O}_2$  battery studies, carbon-based materials, either alone or with some catalysts, are used as cathodes [47–51] because of their high conductivity, high surface area, high porosity, light weight and good oxygen reduction reaction (ORR) activity. Super P, ketjen black, [52–56] carbon nanotubes, [57–60] and graphene [61–63] are some of the carbon-based materials that have been studied in  $\text{Li-O}_2$  batteries, where carbon enables superior gravimetric capacity owing to its aforementioned properties.

Although it is an advantageous cathode material for  $\text{Li-O}_2$  batteries, carbon is not a very stable in the the battery operation environment and is prone to severe decomposition. Studies show that carbon based cathodes oxidize above 4V versus  $\text{Li/Li}^+$  [64] and it also decomposes due to the attack of intermediate products. [65] There is considerable number of studies investigating the mechanism of carbon cathode degradation in  $\text{Li-O}_2$  batteries. McCloskey et al. [66] studied the

stability of various carbon materials in Li-O<sub>2</sub> batteries and indicated that Li<sub>2</sub>O<sub>2</sub> is metastable when in contact with carbon and chemically react with carbon to form Li<sub>2</sub>CO<sub>3</sub>. Gallant et al. [65] suggested that even if the crystalline Li<sub>2</sub>CO<sub>3</sub>, which is formed after first discharge, can be entirely removed after subsequent charge; it becomes difficult to oxidize it at further cycles. In accordance with these studies, Thotiyl et al. [48] suggested that on discharge, dominant product is Li<sub>2</sub>O<sub>2</sub> and electrolyte decomposition is another major reason for side product formation. They also showed that in charge, even if carbon cathode is stable up to 3.5 V, at higher voltages, it decomposes to form Li<sub>2</sub>CO<sub>3</sub> and other similar side products. In these studies it was shown that, upon cycling, accumulation of side products arises and eventually results in capacity fading. For this reason, improvement of capacity retention in Li-O<sub>2</sub> batteries might only be possible if the side reactions are effectively blocked with stable cathodes and electrolytes.

The apparent stability problem of carbon, pushed many researchers to find non-carbon alternatives of cathode materials for Li-O<sub>2</sub> batteries. Cobalt, [67–69] ruthenium, [70–72] and titanium [73, 74] based metals and oxides are some of the most widely used non-carbon materials for Li-O<sub>2</sub> battery cathodes. In these studies, improved number of battery cycles are achieved, however since the cathodes are much heavier than carbon, gravimetric capacities were found to be significantly lower when compared to the theoretical capacity of Li-O<sub>2</sub> batteries. For instance, Peng et al. [75] achieved 95% capacity retention up to 100 cycles by using a nanoporous gold cathode but the capacity achieved is merely 300 mAhg<sup>-1</sup>. Thotiyl et al. [76] reported another study by using TiC as a non-carbon cathode. Experiments revealed that TiC based cathode greatly reduced side reactions and showed excellent cycling performance but the gravimetric capacity of the cathode was again inevitably poor (>98% capacity retention after 100 cycles at a capacity of 350 mAhg<sup>-1</sup>). They interestingly showed that TiO<sub>2</sub> rich surface layer that is presented on the TiC particles was responsible for the excellent performance of the cathode. Adams et al. [77] later reported the importance of the thickness of this TiO<sub>2</sub> layer, as it might block the electron transfer to the surface reactions even if it is as thin as 3 nm, so they suggested to keep it below a critical thickness of around 2 nm.

## 1.4 Motivation

In this thesis study, we aimed to exploit the advantages of carbon as a cathode material for Li-O<sub>2</sub> batteries, while increasing its stability against harmful side reactions. In order to achieve this, multiwalled carbon nanotubes (CNTs) are coated with an ultrathin (sub-nanometer) conformal TiO<sub>2</sub> protective layer via self-limiting atomic layer deposition (ALD) method.

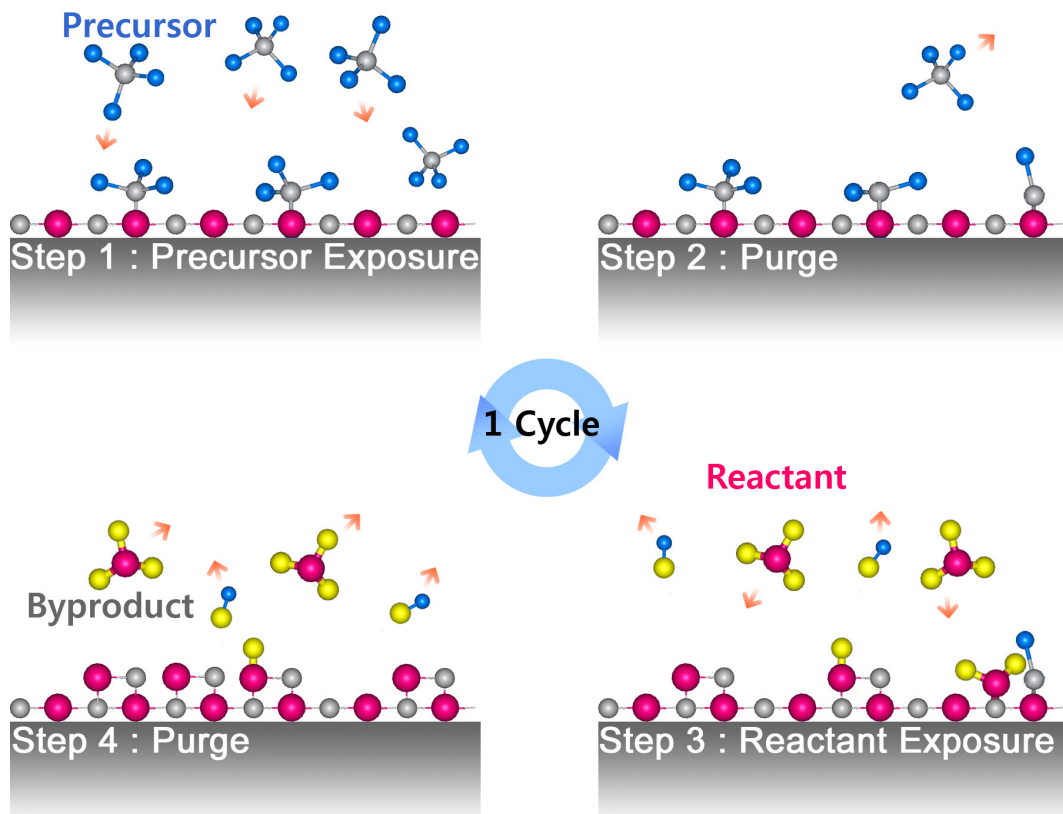


Figure 1.8: A schematic representation of one ALD cycle. [78]

ALD is a chemical thin film deposition technique. The film deposition is realized with sending gaseous precursor to the substrates like chemical vapor deposition (CVD) technique. In contrast to CVD, the precursor is not send to the deposition chamber all at once but sequentially within cycles. In each cycle, the pulsed precursor gas reacts with the substrate surface in a self limiting manner. This unique property enables highly uniform coatings even on very complex substrate surfaces. Furthermore, by varying the cycle numbers, very

precise control on coating thickness is possible with ALD. [79, 80] As can be seen from Figure 1.8, one ALD cycle consist of four main steps: 1) precursor gas exposure, 2) evacuation or purging of the precursors and any byproducts from the chamber, 3) exposure of the other reactant species and 4) evacuation or purging of the reactants and byproduct molecules from the chamber.

The protective  $\text{TiO}_2$  layer that is deposited via ALD, provides a stable interface for the electrochemical reactions while preventing side product formations due to interactions between cathode and electrolyte at high voltages. With the few monolayer thick  $\text{TiO}_2$  coated cathode structure, side product formation caused by carbon decomposition is effectively reduced and excellent full-capacity cycling has been achieved for a carbon-based cathode. The coating properties and thickness are supported by transmission electron microscopy (TEM) imaging. The stability of the cathode is supported by x-ray photoelectron spectroscopy (XPS) analyses and scanning electron microscopy (SEM) imaging.

# Chapter 2

## Materials and Methods

### 2.1 Materials

#### 2.1.1 Cathode and Electrolyte Preparation

Multiwalled carbon nanotubes (CNTs) were used as base cathode material in the Li-O<sub>2</sub> batteries. CNTs were purchased from ALDRICH (724769 ALDRICH O.D. x L 6-9 nm x 5  $\mu$ m, >95% carbon) and used without further purification. CNTs were casted onto nickel foam (Ni-foam) to enable better oxygen diffusion through cathode and to increase the actively used surface area. Prior to usage, Ni-foams were washed with dish-washing liquid containing water in order to remove organic residues. After washing they rinsed with deionized water, ethanol and acetone and finally dried in furnace at 60°C. CNTs were coated with TiO<sub>2</sub> layer by ALD method, which will be explained in detail below. As received CNTs have hydrophobic inert surfaces however ALD coating necessitate hydrophilic surfaces with functional groups to initiate interaction between the surface and the precursor. That is why the purchased CNTs are treated with different surface modification methods in order to open functional groups onto inert CNT surfaces to enable ALD coating. The surface modification methods will be explained in details in the following subsection.

Lithium bis-trifluoromethanesulfonimide-tetraethylene glycol dimethyl ether (LiTFSI-4G) was used as ether based electrolyte. 4G was dried with molecular sieves in glovebox ( $O_2 < 0.5$  ppm,  $H_2O < 0.5$  ppm) before electrolyte preparation and it has  $<5$  ppm  $H_2O$  content. Prior to that, molecular sieves were regenerated in tube furnace in argon atmosphere at  $250^\circ\text{C}$  for 8 hours and take into glovebox. 5 molar electrolyte was prepared by mixing LiTFSI with 4G in glovebox.

#### 2.1.1.1 Surface Modification

Four different surface modification methods were tried: Plasma ashing, Cetyl trimethylammonium bromide (CTAB) and acid functionalization.

Plasma ashing was done with Asher device before  $TiO_2$  coating in oxygen and nitrogen environment for varying time periods. Before surface modification a CNT solution was prepared by mixing isopropanol with as received CNT powder and nafion binder (Dupont DE520 Nafion®). The solution was sonicated with ultrasonic bath and stirred with magnetic stirrer until obtaining a homogeneous CNT solution. The obtained solution then was cast onto Ni-foam and dried in furnace at  $60^\circ\text{C}$ .

For CTAB surface modification, a deionized water solution was prepared with 1 wt% CTAB powder. The solution was mixed with as received CNT with 1 g/L ratio. The final solution was then sonicated with ultrasonic bath for 1 hour. After the sonication the mixture was centrifuged 5 times in order to remove the residuals. The remaining powder was then dried in furnace at  $60^\circ\text{C}$ . Finally a solution was prepared with remaining CTAB functionalized CNT (fCNT(CTAB)) powder, isopropanol and nafion binder and casted onto Ni-foam as explained before.

For acid functionalization, as received CNTs were added to  $HNO_3/H_2SO_4$  (1:3) solution. The solution was mixed with magnetic stirrer at  $70^\circ\text{C}$  for 2 hours. Afterwards 5% HCl was added to the mixture. The final solution was vacuum filtered and simultaneously washed with deionized water for several times. The fCNTs

were dried at 60°C for several days. A solution was prepared with acid functionalized CNTs (fCNT(acid)), isopropanol and nafion binder and the solution was casted onto Ni-foams.

#### **2.1.1.2 TiO<sub>2</sub> Coating with ALD and Annealing**

The obtained fCNT-Ni-foam samples were coated with TiO<sub>2</sub> by using Savannah S100 ALD reactor (Ultratech Inc.). The substrate temperature was kept at 150°C during ALD process using Ti(NMe<sub>2</sub>)<sub>4</sub> and H<sub>2</sub>O as titanium and oxygen precursors, respectively. Before deposition, Ti(NMe<sub>2</sub>)<sub>4</sub> precursor was pre-heated to 75°C for sufficient vapor pressure and N<sub>2</sub> was employed with a flow rate of 20 sccm as the carrier gas. After TiO<sub>2</sub> coating, cathodes were annealed using a tube furnace in argon atmosphere. Samples were subjected to argon flow for 30 minutes for purging the tube prior to annealing. Samples that were functionalized with CTAB heated up to 650°C at a rate of 3°C/min. After waiting 1 hour at 650°C and then left to cool down. Samples that were functionalized with acid heated up to 450°C at a rate of 5°C/min and be waited at 450°C for 30 minutes. The annealed cathodes were denoted as "-Ann" after the name of the specific cathode.

### **2.1.2 Li-O<sub>2</sub> Battery Cell Configuration**

Li<sub>2</sub>O<sub>2</sub> batteries were prepared in glovebox in argon atmosphere without exposing the air environment. A Swagelok type battery cell is used. Pure Li metal (Sigma Aldrich) used as anode material. Celgard and Glassfiber C (Whatman) were used as separators. 0.5 M LiTFSI-4G was used as ether based electrolyte. TiO<sub>2</sub> coated multiwalled carbon nanotubes were used as cathode material. The battery cell and inner components were first washed and then rinsed with deionized water, ethanol and acetone respectively. After drying the battery cell, the inner components and the previously prepared cathode were waited overnight in vacuum furnace at 70°C and then take into the glovebox. A schematic representation of

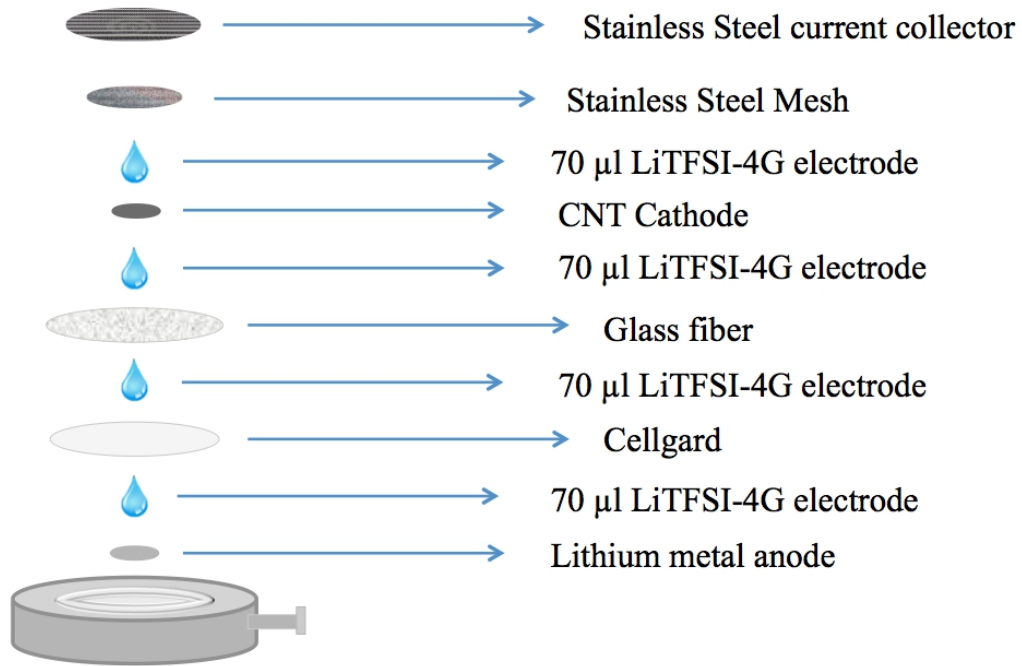


Figure 2.1: Schematic representation of Li-O<sub>2</sub> battery cell configuration.

the battery configuration is shown in Figure 2.1. A stainless steel mesh was used for oxygen gas diffusion and another stainless steel current metal was used for current collector. Prepared batteries were rested for 8 hours and then filled with ultra pure oxygen gas (0.5 bar) before electrochemical testing.

## 2.2 Characterization

Throughout the thesis study several characterization devices were used to investigate the various properties. Cathodes were characterized before and after battery operations. FEI Tecnai G2 F30 Transmission Electron Microscopy (TEM), FEI Quanta 200 FEG Environmental Scanning Electron Microscope (SEM), Thermo Scientific X-ray Photoelectron Spectrometer (XPS) and PAN analytical XPert X-ray Diffractometer with Cu K $\alpha$  radiation (XRD) were the used characterization devices.

The  $\text{TiO}_2$  coated CNTs were visualized by TEM. In order to prepare TEM sample, a small piece of the cathode sample was taken and put in a glass vial which is filled with pure isopropanol. The vial was sonicated in ultrasonic bath for 30 minutes. After the sonication a little amount of the solution was dropped onto copper grid with micro pipette and air dried.

Pristine and battery cycled cathodes were also visualized with SEM. Batteries that finished the operation were disassembled in glovebox and the cycled cathodes were taken out. The cycled cathodes were washed in glovebox with acetonitrile ( $<3$  ppm water content) and let to dry in glovebox for further analyses. The cycled cathodes then carried to SEM chamber with an argon filled airtight container.

Pristine and battery cycled cathodes were also analyzed with XPS to investigate the stability of the cathodes. The sample preparation of cycled cathodes for XPS is exactly same with SEM.

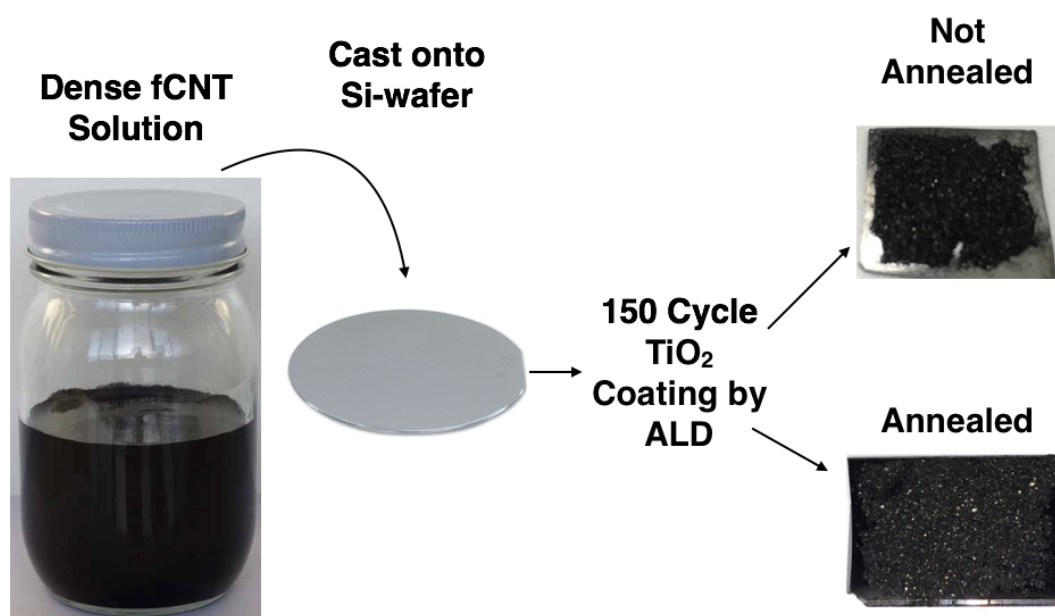


Figure 2.2: XRD sample preparation scheme for analyzing the crystallization of  $\text{TiO}_2$  after annealing.

In order to investigate crystallization properties of the TiO<sub>2</sub> coated CNTs XRD analyses were carried out. Firstly a thick solution is prepared with previously acid functionalized CNT and isopropanol. The solution was then casted onto a silicon wafer (Si-wafer) and dried in the furnace at 60°C. The CNT-Si-wafer sample then TiO<sub>2</sub> coated by ALD. The coated sample was then annealed with the same conditions used for battery cathodes, while one TiO<sub>2</sub>-CNT-Si-wafer sample left without annealing for comparison. Finally, the prepared samples were analyzed with XRD before and after annealing. A schematic representation of XRD sample preparation is shown in Figure 2.2

## 2.3 Electrochemical Tests

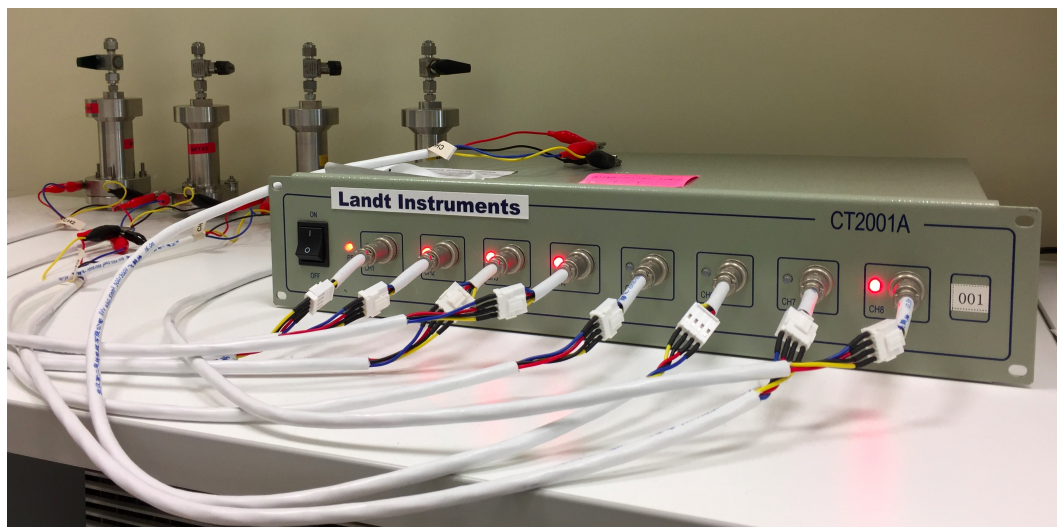


Figure 2.3: Landt CT2001 multichannel potentiostat/galvanostat.

Electrochemical tests were conducted with Landt CT2001 multichannel potentiostat/galvanostat (Figure 2.3) at 100 mA<sup>g</sup><sup>-1</sup> current rate between 2 to 4.5 V potential window. The average cathode mass is 0.7 mg which is the weight of CNT and TiO<sub>2</sub> in the cathode.

The battery tests were conducted through full capacity discharge and charge cycles. The batteries were either subjected to one discharge and charge cycle to investigate the initial capacity or subjected to 5 or 20 full capacity discharge and charge cycles to investigate the capacity retention of the relevant cathodes.

In addition to battery tests, cyclic voltammetry (CV) and impedance spectroscopy tests were performed via Biologic SP-150 electrochemistry instrument. CV measurements were performed between 2 to 4.5 V, 0.5 mV/s scan rate for 2 cycles at room temperature (RT). Impedance measurements were performed on open circuit potential between 0.1 Hz to 1MHz with 10 mV oscillation potential at RT.

# Chapter 3

## Results and Discussion

In this thesis study, a stable cathode material is produced for Li-O<sub>2</sub> batteries. The study undergone three main progression steps that each one follow the other. The motivation is to build up a carbon based cathode material that can withstand degradation upon battery cycling. Carbon based materials, in our case carbon nanotubes (CNT), have many advantages as a cathode material in Li-O<sub>2</sub> batteries such as high surface area, high porosity, high electrical conductivity, lightweight and very good oxygen reduction reaction activity. However they are very unstable in Li-O<sub>2</sub> battery environment especially upon battery cycling. To be able to benefit from the appealing advantages of CNTs in a longer time scale, a protective TiO<sub>2</sub> layer was coated on the surface of CNTs by atomic layer deposition (ALD) method.

In this chapter, the production steps, battery performance and the stability of the mentioned cathode materials were explained and discussed under three separate sections: 3.1 CNT Surface Modification, 3.2 Optimization of TiO<sub>2</sub> Coating and 3.3 Stability Tests of Li-O<sub>2</sub> Battery Cathode.

In the first section, three different CNT surface modification techniques were discussed with TEM images and battery results. CNTs necessitate a surface modification step prior to TiO<sub>2</sub> coating in order to open up functional groups that molecules can attach to. At first plasma ashing method was tried for surface modification however this method was found to be unreliable since a consistent coating could not be obtained on several different coating conditions of ALD. Secondly CTAB surface modification method was tried, which is a surfactant material that absorbs on the CNT surface and lowering the surface energy. Even though some promising results were obtained with this surface modification method, it was then realized that the method was not stable against annealing and also some residues can not be washed away after the surface modification. Finally an acid functionalization method was tried as a surface modification. Fortunately very promising results could be obtained from this method even with very few ALD cycle coatings.

In the second section, the optimization of TiO<sub>2</sub> coating was discussed. Several ALD cycles had been tried from 100 cycles to 1 cycle. With decreasing the ALD cycles coating thickness was decreased and battery capacity was increased. The optimum one was found to be 5 ALD cycles with sub-nm TiO<sub>2</sub> coating.

In the final section the stability of the produced cathodes was investigated by XPS characterization and SEM imaging of before and after battery cycling. Consequent characterization results proved that TiO<sub>2</sub> coating indeed lowered side product formations on cathode electrolyte interface upon battery cycling and increase the stability compared to bare CNT.

## 3.1 CNT Surface Modification

Surface modification is basically introducing chemical functional groups into a surface. By surface modification, various properties of the materials like roughness, [81] hydrophilicity, [82] surface charge, [83] reactivity [84] etc. can be modified.

Since its discovery CNT attracted huge amount of attention from the fields of nanotechnology, electronics, optics to material science and energy thanks to its extraordinary electrical, thermal, mechanical and optical properties. [85–87] However CNTs almost exclusively necessitate a prior surface modification process to benefit from its properties which are hindered by their intrinsic poor solubility and processability. [88] Surface modification of CNTs can either be performed via chemical methods or non-covalent wrapping methods. [89–91] In this particular study, as mentioned before, the idea was to coat CNTs with a uniform  $\text{TiO}_2$  protective layer by ALD to prevent side product formation happening on cathode electrolyte interface. However CNTs have hydrophobic surfaces so they lack functional groups for film deposition to happen. To overcome this problem, surface modification methods were performed to as received CNTs. In this section the performed surface modification techniques will be discussed and the representative coating results will be presented.

### 3.1.1 Plasma Ashing

Plasma ashing is a surface treatment technique. In this technique a plasma source is used to generate so called reactive species and these reactive species are sent to the treated surface to open up functional groups. [92] Plasma ashing is generally used for photoresist removal in semiconductor manufacturing. [93, 94]

Plasma ashing was performed to CNT-Ni-foam samples before  $\text{TiO}_2$  coating. The cathode that functionalized with plasma ashing (P) and 100 ALD cycles of  $\text{TiO}_2$  (100T) coating (P-100T) had been tried. TEM images of the P-100T are

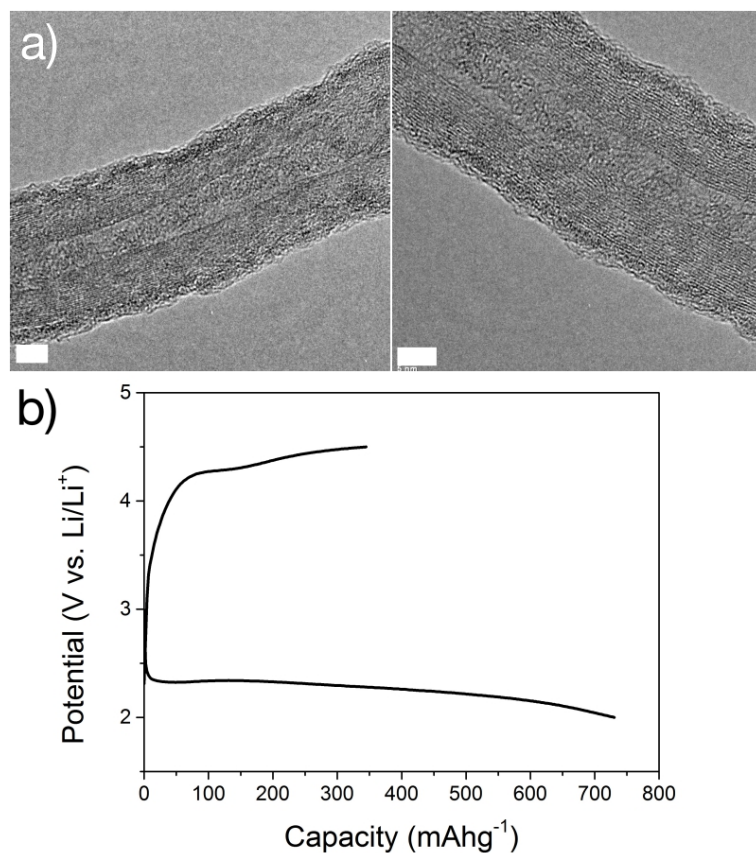


Figure 3.1: a) TEM Images of P-100T cathodes. White bars indicate 5 nm in scale, b) Battery performance of P-100T cathode at  $100 \text{ mA g}^{-1}$  current rate.

presented in Figure 3.1a). As can be seen from the figure, successful coating of 2-5 nm  $\text{TiO}_2$  was obtained, however the cathode showed a rather low capacity at  $100 \text{ mA g}^{-1}$  current rate as can be seen from Figure 3.1b). This was most probably because the low electrical conductivity of comparatively thick amorphous  $\text{TiO}_2$  layer. [95]

In order to increase the capacity, lesser ALD cycles decided to be tried. At first 25T decided to be tried however a successful coating couldn't be achieved as can be seen from Figure 3.2. The first idea that come to mind was the ALD cycles weren't enough and an optimum cycle number need to be found to achieve in order to have a very thin and uniform coating.

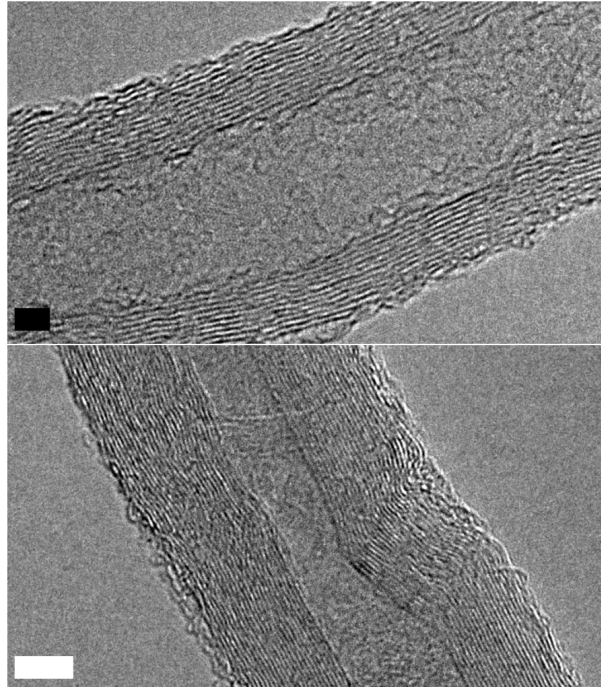


Figure 3.2: TEM Images of P-25T cathodes. White bar indicate 5 nm and black indicate 2 nm in scale respectively.

Then 50T decided to be tried. A couple of TEM images is presented in Figure 3.3. Even though ALD cycle number was doubled, CNT surfaces seem to be bare which means again there was no coating.

The battery test of P-25T and P-50T cathodes also had been performed which are presented in Figure 3.4. P-25 and P-50 cathodes showed higher capacities compared to P-100 cathode due to increased conductivity but since the coating didn't happen they wouldn't be stable against battery cycling.

At this point it was decided to adjust the parameters of plasma ashing to be able to induce more proper surface modification. On the previous surface modifications 2 minutes of plasma ashing was performed. It had been decided to increase the surface modification time. However doing plasma ashing more than 2 minutes resulted in material loss by CNT burn out and detaching from Ni-foam. This being the case, over surface treatment possibility is considered and it had been decided to decrease the plasma ashing time. To enable a reasonable comparison, P-75T with 2, 1,5 and 1 minutes of plasma ashing were tried. In

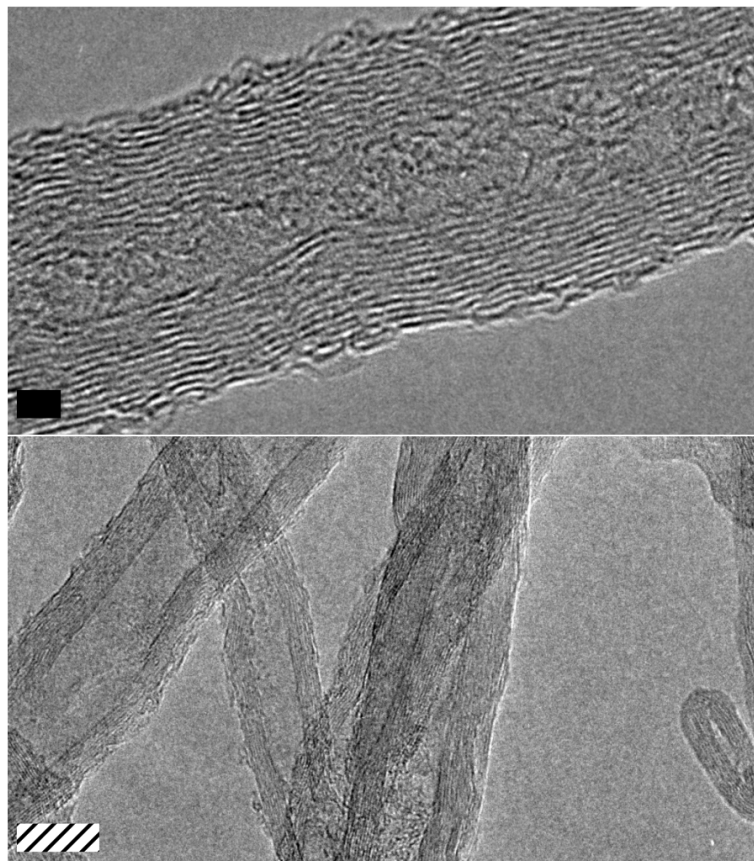


Figure 3.3: TEM Images of P-50T cathodes. Black bar indicate 2 nm and dashed bar indicate 10 nm in scale respectively.

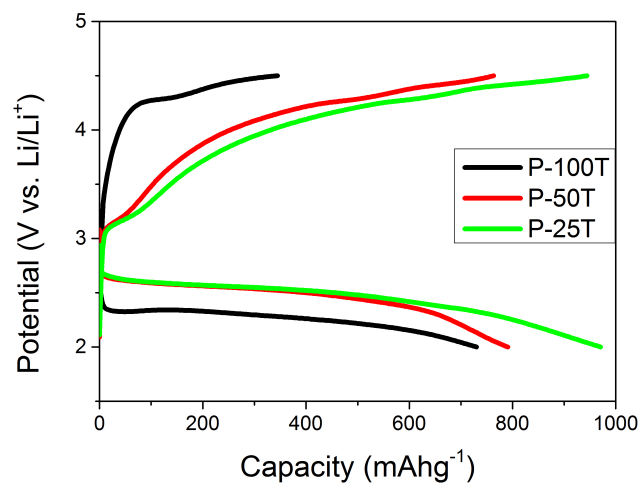


Figure 3.4: Battery performance comparison of P-100T, P-50T and P-25T cathodes at 100 mA<sub>g</sub><sup>-1</sup> current rate.

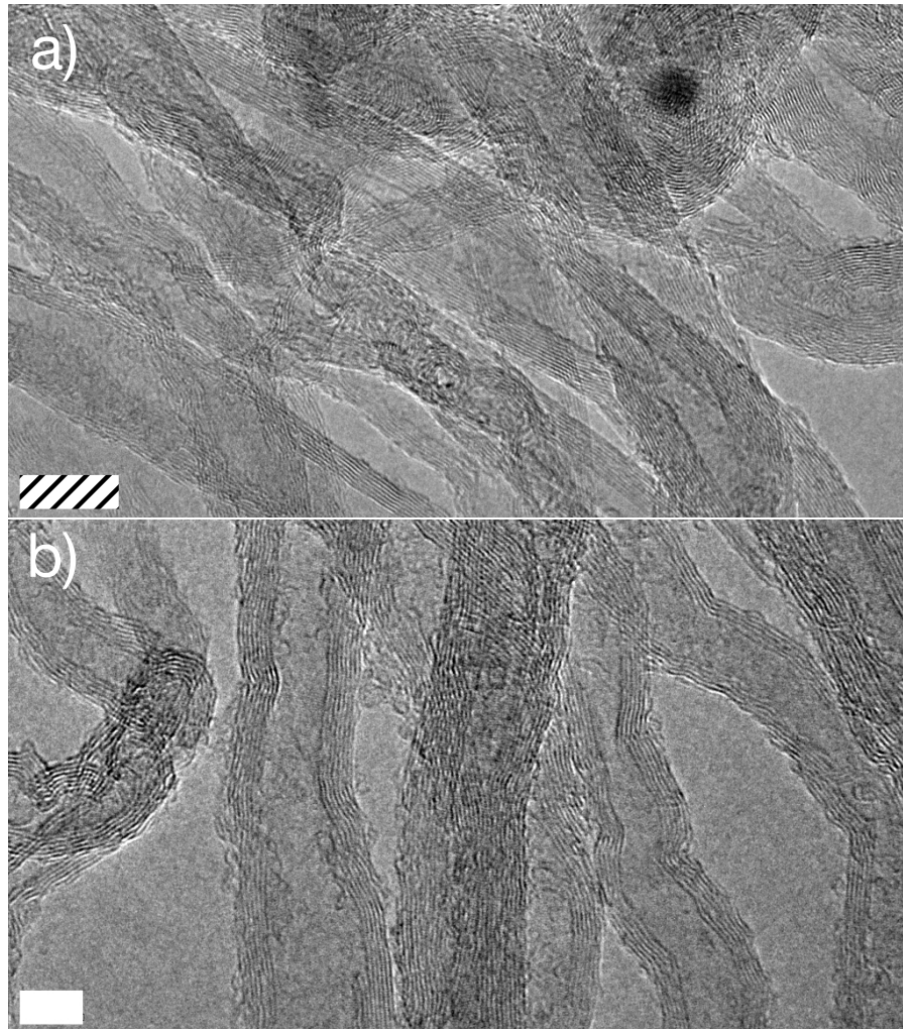


Figure 3.5: TEM images of P-75T cathodes at a) 1,5 and b) 2 minutes of plasma ashing. Dashed and white bars represent 10 and 5 nm respectively.

Figure 3.5 the TEM images of these samples are shown. Unfortunately a proper TEM image of 1 minute plasma ashed sample couldn't be obtained, nevertheless, a successful coating did not happen neither for 2 nor for 1.5 minutes plasma ashed samples. It finally had been decided that plasma ashing was not a consistent and reliable surface modification method and another method decided to be applied for CNT surface modification.

### 3.1.2 CTAB Surface Modification

CTAB (Cetyl trimethylammonium bromide,  $(C_{16}H_{33})N(CH_3)_3Br$ ) is a quaternary ammonium surfactant. It is commonly used in chemical and biological synthesis. CTAB is adsorbing to the target surface and lowering the surface energy. [96].

After the surface modification of CNTs with CTAB as explained in materials and methods section, C-25T, C-50T, C-75T and C-100T cathodes were prepared by coating with 25, 50, 75 and 100 ALD cycles of  $TiO_2$  respectively. As can be seen from Figure 3.6a, b and c),  $TiO_2$  was grown on C-25T, C-50T and C-75T cathodes as nanoparticles rather than a uniform coating. Dark field TEM images more clearly demonstrate the nanoparticle like formations. Only in C-100T cathode a considerable  $TiO_2$  coating was obtained with some partially not coated regions.

Battery cycling test of these cathodes were also performed. In Figure 3.7 first discharge and charge curves of these cathodes are shown. Additionally battery test of bare CNT cathode was also performed for comparison. The coated cathodes showed considerably reasonable and similar capacities however lower than CNT cathode since it has a lower weight and higher electrical conductivity. Even though CTAB residues were cleaned several times with deionized water after the surface modification, as explained in Materials and Methods chapter, there might be some remaining, which is the reason of extra weight apart from  $TiO_2$  coating. It is important to mention that coated cathodes showed noticeably lower over-potential compared to CNT cathode, which can be explained with catalytic effect of  $TiO_2$ . Nevertheless it is safe to say that all four coated cathodes showed comparable battery performances.

As deposited  $TiO_2$  was in amorphous form since the deposition was performed under the crystallization temperature of  $TiO_2$ . [97] In order to increase the electrical conductivity, it was decided to introduce an annealing step to the cathode preparation to obtain a crystalline  $TiO_2$  phase. One pair of C-50T and C-100T cathodes were prepared. The cathodes were then annealed at  $650^\circ C$  as explained

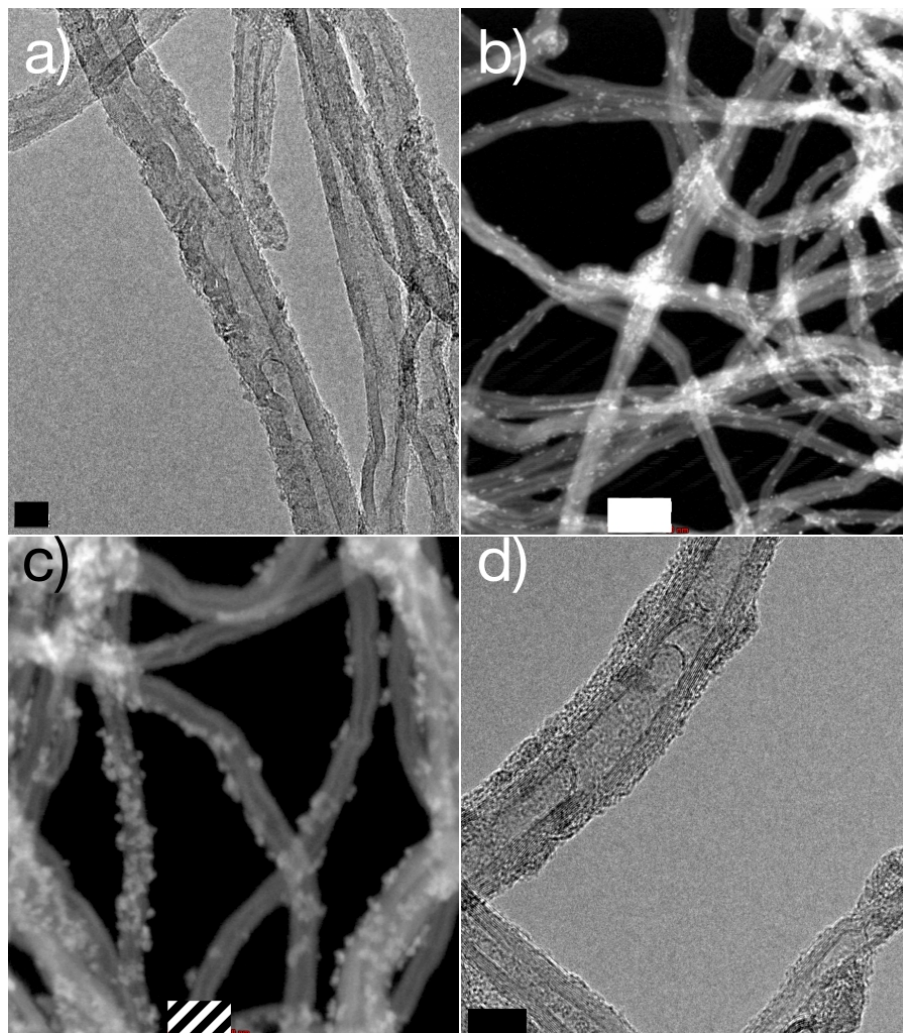


Figure 3.6: TEM images of a) C-25, d) C-100 and Dark field TEM images of b) C-50 and c) C-75 cathodes. Black, dashed and white bars indicate 10, 50 and 20 nm in scale, respectively.

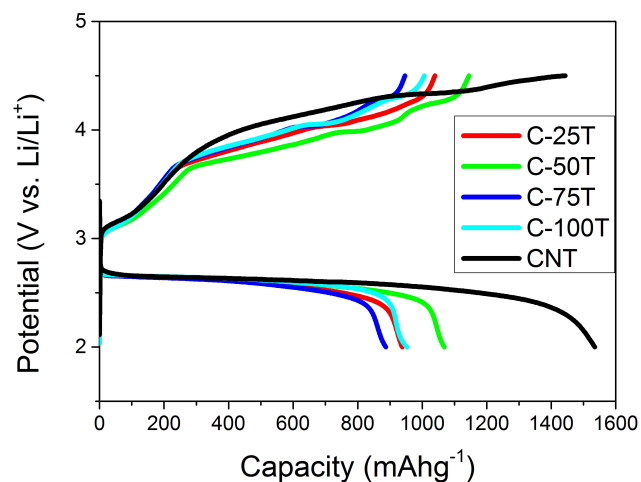


Figure 3.7: Battery performance comparison of C-25, C-50, C-75, C-100 and bare CNT cathodes.

in Materials and Methods chapter, which are denoted as C-50T-Ann and C-100T-Ann, respectively. TEM images of these cathodes were taken before and after annealing procedure (Figure 3.8) Previously prepared P-100T sample was also annealed with same parameters to compare the effect of the annealing to CTAB and Plasma Ashing functionalized  $\text{TiO}_2$  coatings.

As presented in Figure 3.8,  $\text{TiO}_2$  coating on C-50T and C-100T cathodes came off and agglomerated into big nanoparticles after annealing. This means  $\text{TiO}_2$  was not firmly absorbed to the CNT surface and not stable at the annealing temperatures. In the case of P-100T-Ann cathode (Figure 3.8f)),  $\text{TiO}_2$  coating was almost preserved. It is worth noting that, for all samples  $\text{TiO}_2$  annealing was happened considering the visible crystalline epitaxial layers.

The reason behind the agglomeration of  $\text{TiO}_2$  after annealing was probably CTAB itself. The surfactant that was absorbed on CNT surface was lifted off after annealing with the coated  $\text{TiO}_2$ , which then agglomerate into spherical particles. The comparatively stable  $\text{TiO}_2$  after annealing on plasma ashing functionalized CNT, support this idea. In order to create a clearer image of the behavior of CTAB functionalized  $\text{TiO}_2$  coated cathodes on annealing, a couple of additional outlook TEM images are given in Figure 3.9. As can be seen from the figure,

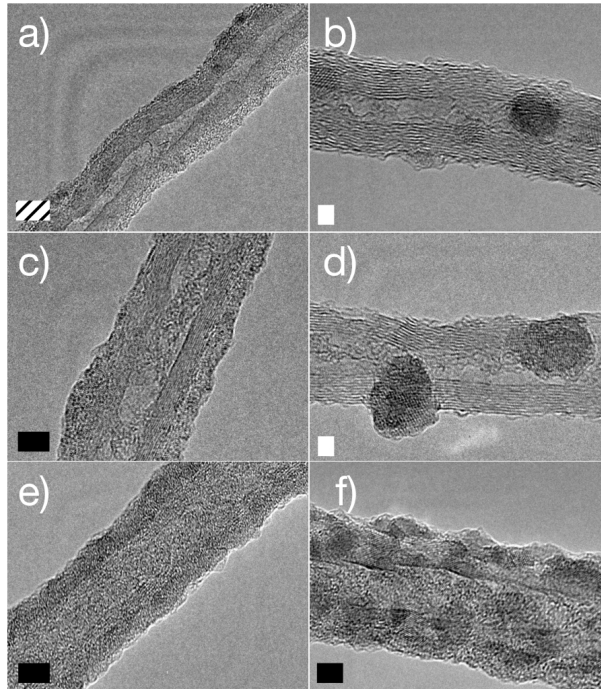


Figure 3.8: TEM images of various cathodes before and after annealing: a) C-50T, b) C-50T-Ann, c) C-100T, d) C-100T-Ann, e) P-100T, f) P-100T-Ann. Dashed, black and white bars indicate 10, 5 and 2 nm in scale respectively.

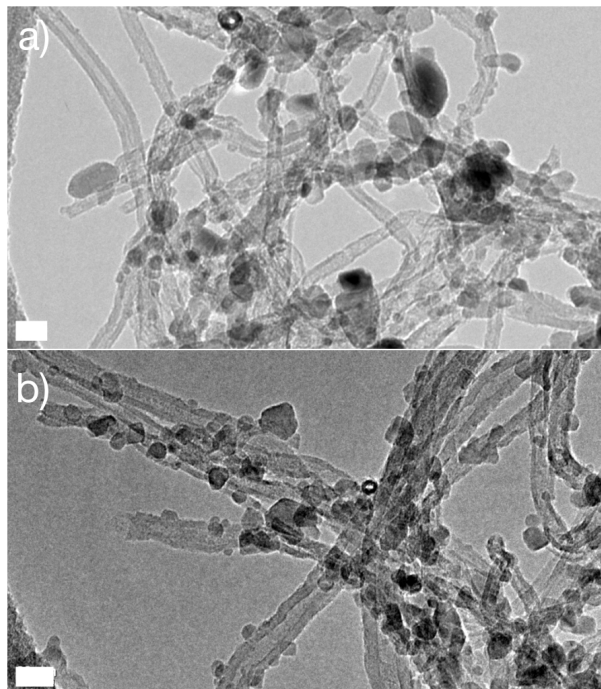


Figure 3.9: TEM images of a) C-50T-Ann and b) C-100T-Ann cathodes. White bars indicate 10 nm in scale.

TiO<sub>2</sub> forms big agglomerates after annealing.

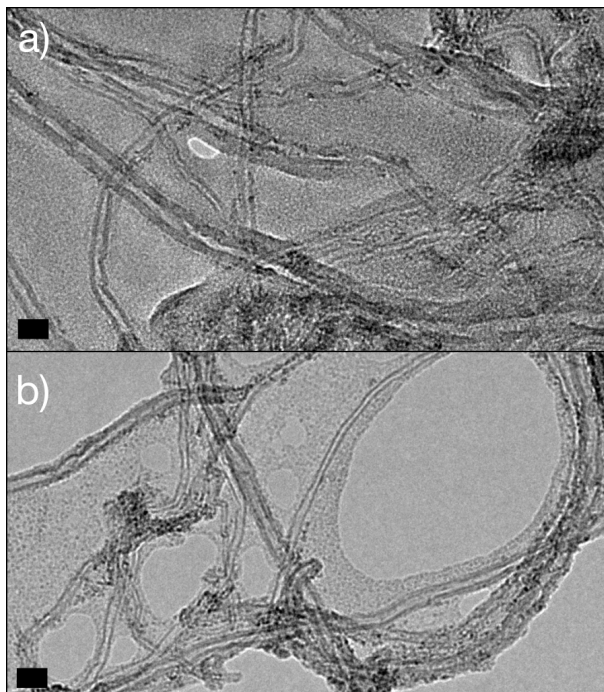


Figure 3.10: TEM images of sheet like layers in between CNTs of a) C-50T and b) C-100T cathodes. Black bars indicate 20 nm in scale.

One other problem that encountered was sheet like layer formation of CTAB between CNT structures as shown in Figure 3.10 This layer was most probably CTAB residue and would lead to unwanted and indeterminable side product formation upon battery cycling. These are being the case, CTAB surface modification was considered unsuccessful and it had been decided to move on to another the surface modification method.

### 3.1.3 Acid Functionalization

Functionalization of CNTs with the treatment of strong acids is a very common surface modification method that used for many years. [98–100] It is basically distorting the surface bonds of CNTs and opening up functional groups as active sites. There are many types of acids that are used for acid functionalization. In this study a solution of HNO<sub>3</sub>/H<sub>2</sub>SO<sub>4</sub> was used. The functionalization method is

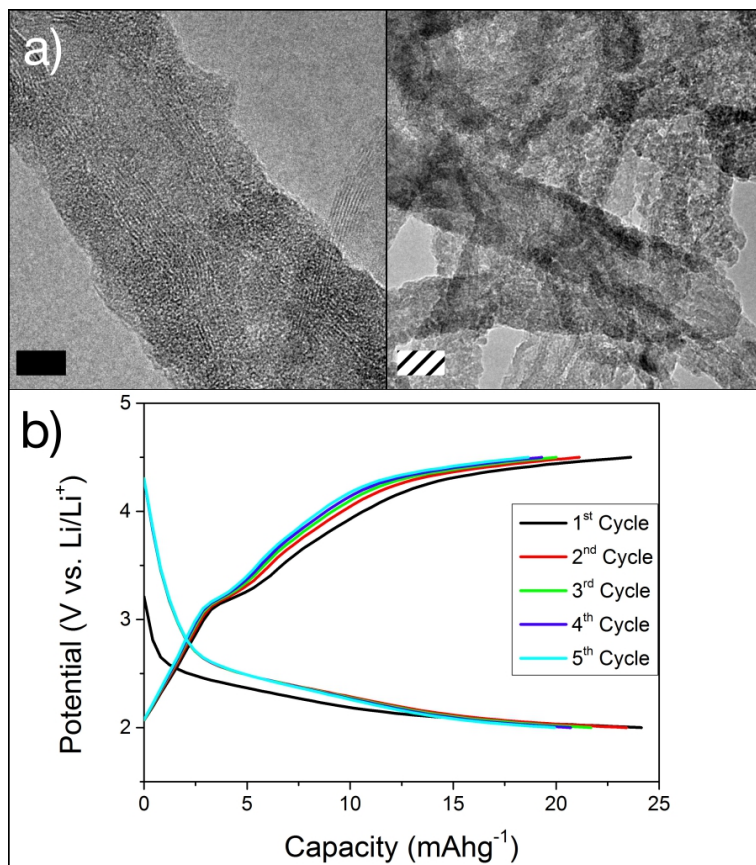


Figure 3.11: a) TEM images of A-100T cathode. Black and dashed bars indicate 5 and 10 nm in scale, respectively. b) Battery cycling performance of A-100T cathode at 100 mA $g^{-1}$  current rate.

described in Materials and Methods chapter in details.

Acid functionalized CNT sample was coated with TiO<sub>2</sub> for 100 ALD cycles (A-100T). In Figure 3.11 TEM images and battery performance of A-100T cathode is given. As can be seen from Figure 3.11a), a rather thick (>5 nm) but a uniform coating was happened throughout CNT surface. The cathode showed a very small battery capacity at 100 mA $g^{-1}$  current rate because of low electrical conductivity of thick TiO<sub>2</sub> layer (Figure 3.11b)). However the capacity retention for 5 battery cycles was quite good, indicating the stable feature of the cathode because of TiO<sub>2</sub> protective layer.

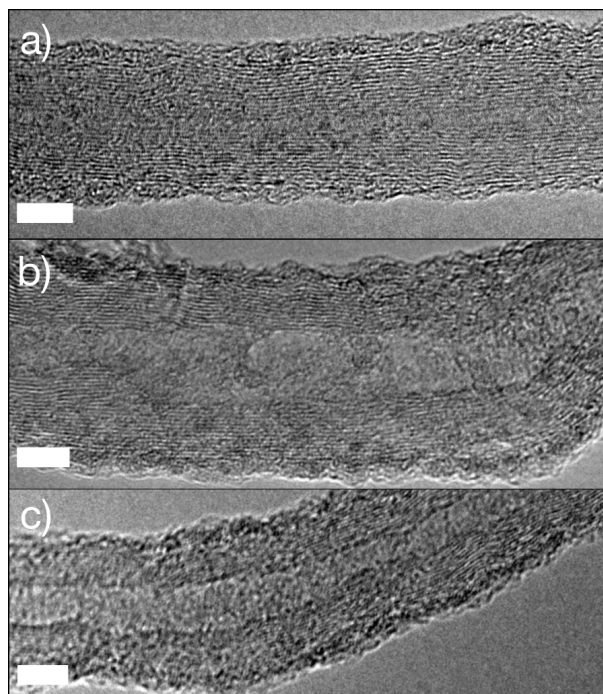


Figure 3.12: TEM images of a) A-50T, b) A-30T and c) A-20T cathodes. White bars indicate 5 nm in scale.

In order to obtain higher battery capacities with lowering the coating thickness, ALD cycles were decreased periodically. In Figure 3.12, TEM images of A-50T, A-30T and A-20T cathodes are given. Considering these three cathodes, the  $\text{TiO}_2$  coating thicknesses are almost same while uniformity of the coating was not affected by decreasing ALD cycles. This is the sign of a successful functionalization process.

## 3.2 Optimization of $\text{TiO}_2$ Coating

Acid functionalized CNT cathodes had been coated successfully with ALD cycles starting from 100 to 20. This shows that acid functionalization was the best choice among the other functionalization techniques. After this point, an optimum coating was tried to be found by investigating the TEM images and battery performances simultaneously.

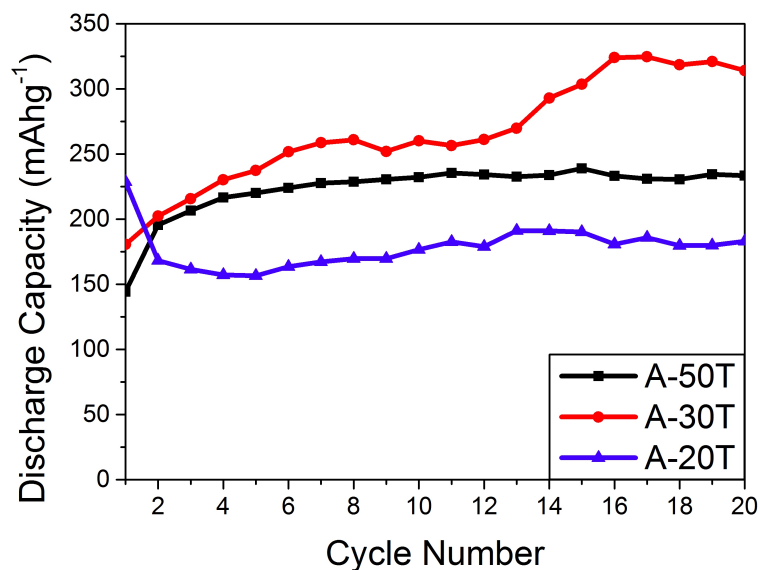


Figure 3.13: Discharge capacity retention comparison of A-50T, A-30T and A-20T cathodes on full 20 discharge and charge battery cycles at  $100 \text{ mA}g^{-1}$  current rate.

In order to see the battery performance of A-50T, A-30T and A-20T cathodes, batteries were prepared and tested. The batteries were subjected to full discharge and charge battery cycling for 20 cycles at  $100 \text{ mA}g^{-1}$  current rate between 2 to 4.5 voltage range. In Figure 3.13 gravimetric capacity retention of these cathodes are presented. As can be seen from the figure, the average capacities of these three cathodes are also very similar. To be more precise, the average capacity of A-30T cathode was increased compared to A-50T cathode ( $270 \text{ mA}h g^{-1}$  vs.  $220 \text{ mA}h g^{-1}$ , respectively) as expected by decreasing the ALD cycles. However the average capacity of A-20T cathode is comparatively lower ( $170 \text{ mA}h g^{-1}$ ), even though the capacity of the first battery cycle was the highest. Nevertheless, since the  $\text{TiO}_2$  coating thickness of the three cathodes are very similar, it is understandable to observe such similar battery capacity values.

The important point here to notice is the capacity retention. All three cathodes showed very good capacity retention behavior on 20 full discharge and charge cycles, which shows the stability of the coated cathodes despite the fact that they still have relatively low capacity values for a  $\text{Li-O}_2$  battery.

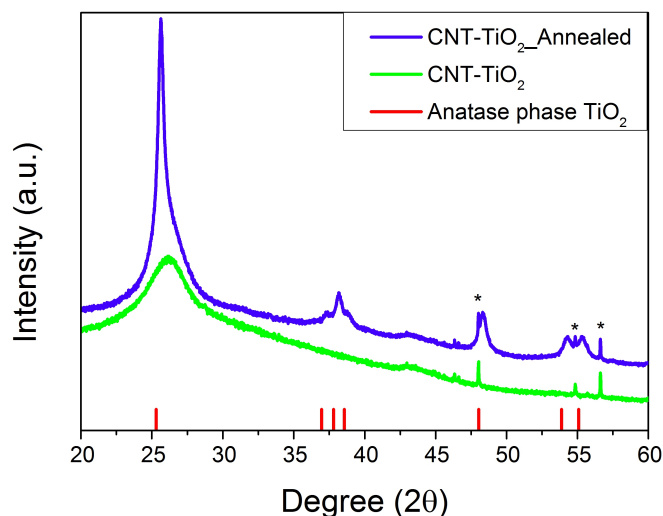


Figure 3.14: XRD pattern of  $\text{TiO}_2$  coated CNTs before and after annealing. CNT- $\text{TiO}_2$  Annealed pattern perfectly matches with Anatase phase  $\text{TiO}_2$  (JCPDS file 21-1272). The peaks that are marked with asterisk are originating from Si-wafer, which the analyzed samples are casted on.

At this point it had been decided to anneal the cathodes to obtain crystalline  $\text{TiO}_2$  coatings alongside CNT surface in order to increase the electrical conductivity and subsequently reaching higher capacity values. This time the annealing parameters had been changed to preserve the uniform coating at the annealing temperatures. In order to do this the annealing temperature decided to be lowered to  $450^\circ\text{C}$  from  $650^\circ\text{C}$  and waiting time to 30 minutes from 1 hour. In order to prove a crystalline phase is obtained after annealing, a separate XRD characterization process was performed. The XRD sample was prepared as it was explained in Chapter 2; a dense solution of isopropanol and previously acid functionalized CNT was prepared and casted onto a silicon wafer (Si-wafer) and dried. The sample was then coated with  $\text{TiO}_2$  by ALD and annealed with the above mentioned parameters, while one  $\text{TiO}_2$ -CNT-Si-wafer sample left without annealing for comparison. In Figure 3.14, the XRD patterns of this samples are given. As can be seen from the XRD patterns, the annealed  $\text{TiO}_2$  transformed to crystalline anatase phase from amorphous phase, which proves the crystallinity after annealing.

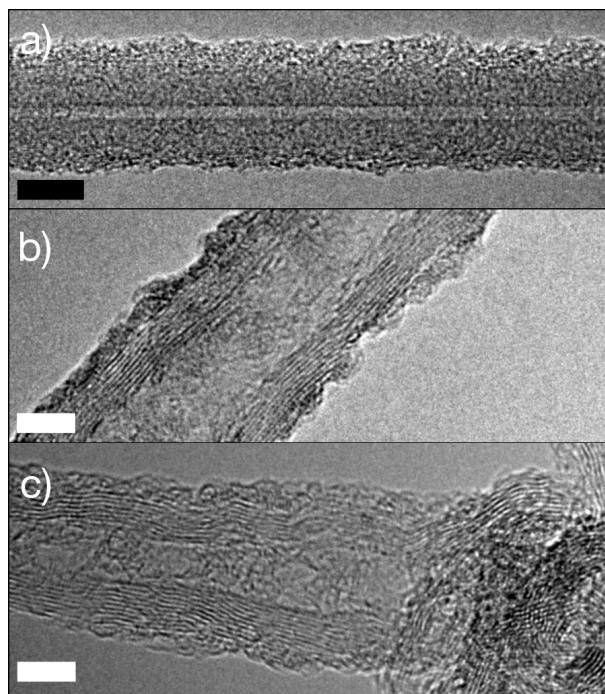


Figure 3.15: TEM images of a) A-50T-Ann, b) A-30T-Ann and c) A-20T-Ann cathodes. Black and white bars indicate 10 and 5 nm in scale, respectively.

TEM images of the A-50T-Ann, A-30T-Ann and A-20T-Ann cathodes are given in Figure 3.15. As can be seen from the figure, uniformity of the  $\text{TiO}_2$  coating was almost completely preserved after annealing. After the annealing process, batteries were prepared with the cathodes and subjected to full discharge and charge battery cycling for 20 cycles at  $100 \text{ mA g}^{-1}$  current rate like previous ones. In Figure 3.16 gravimetric capacity retention of these cathodes are presented. The batteries showed a significant capacity increase as can be seen from the figure. This corresponds to aforementioned electrical conductivity increase of the annealed cathodes due to crystallinity of  $\text{TiO}_2$ . This time A-20T-Ann cathode showed the highest average capacity ( $1200 \text{ mA h g}^{-1}$ ) as expected, which followed by A-30T-Ann ( $600 \text{ mA h g}^{-1}$ ) and A-50T-Ann ( $450 \text{ mA h g}^{-1}$ ) cathodes. Moreover, the capacity retention of the batteries on 20 full discharge and charge cycles are perfect regardless of the capacity value, which again proves the stability of the  $\text{TiO}_2$  coated cathodes.

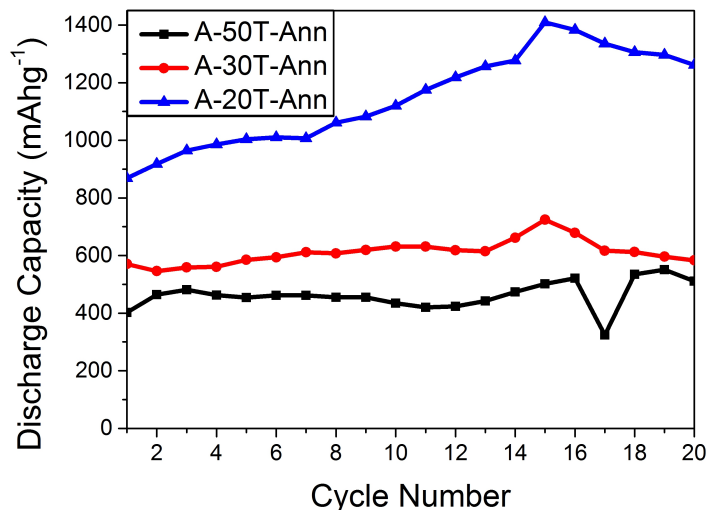


Figure 3.16: Discharge capacity retention comparison of A-50T-Ann, A-30T-Ann and A-20T-Ann cathodes on full 20 discharge and charge battery cycles at 100  $\text{mA g}^{-1}$  current rate.

In these 20 battery cycles there are some sudden or slow but progressive capacity increase or decrease as can be noticed from the Figure 3.16. In order to understand this behavior, first it is important to point out again that the batteries were cycled on full discharge and charge cycles. This means the capacity value at the end of each discharge can not be expected to be same on each cycle. If the capacities follow a straight-like path, as in the case of Figure 3.16, it can be considered as a good capacity retention. Considering the sudden capacity jumps; it is clear that the sudden changes are just for that specific cycles because on the following cycles the capacity line continues where it was left of. The most possible explanation for this behavior is the temperature change in the environment while battery operation. The temperature can affect the battery performance as it is stated in many studies [101–103]. Unfortunately the batteries were operated in an environment that is temperature can not be controlled. However, the overall behavior of the battery was stable.

In the light of good results of decreasing the ALD cycles and annealing, it had been decided go further on. A-10T-Ann, A-5T-Ann and even A-1T-Ann cathodes were prepared. In Figure 3.17 TEM images of A-10T-Ann, A-5T-Ann and

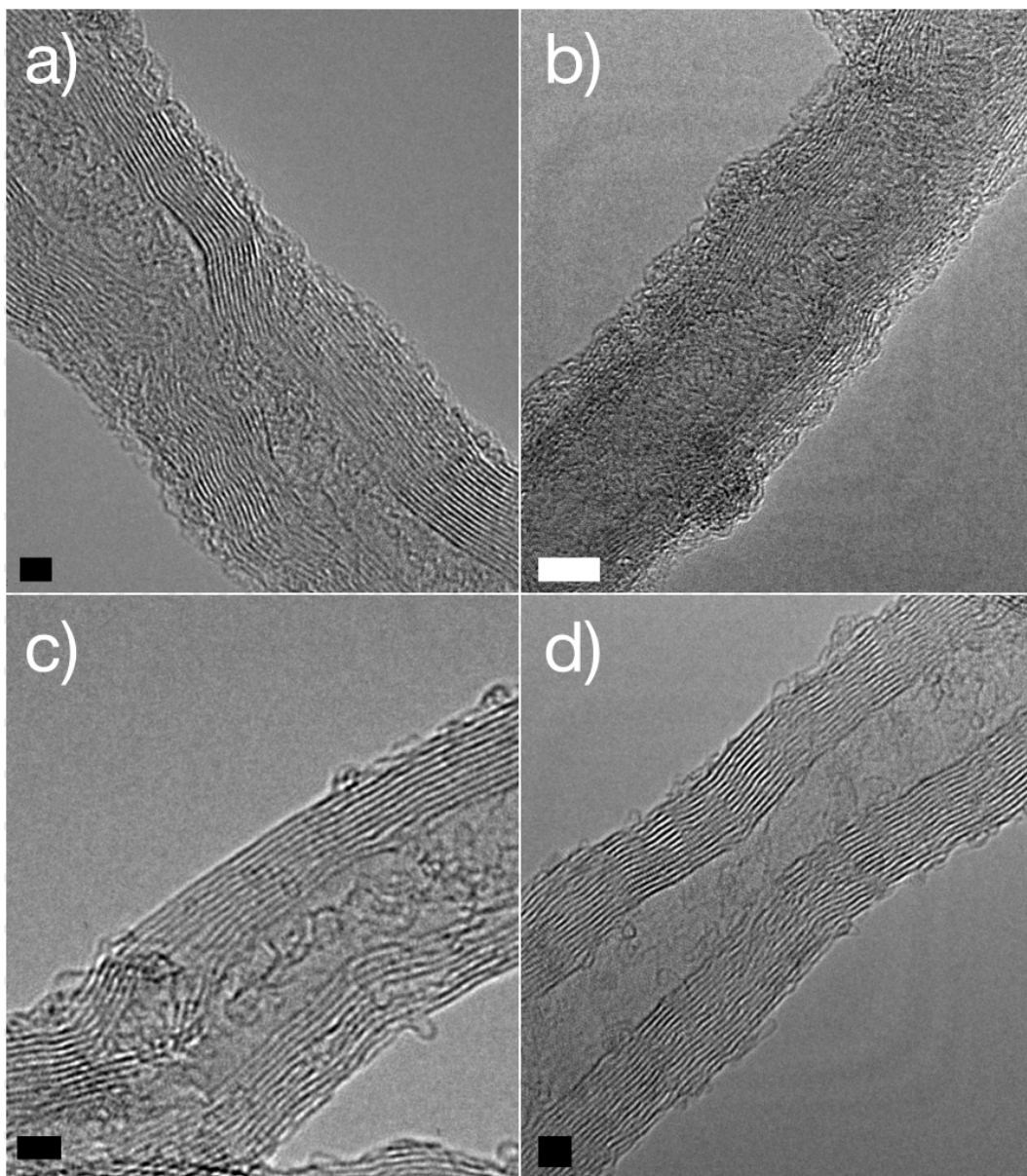


Figure 3.17: TEM images of a) A-10T-Ann, b) A-5T-Ann, c) A-1T-Ann and d) Acid functionalized CNT. Black and white bars indicate 2 and 5 nm in scale, respectively.

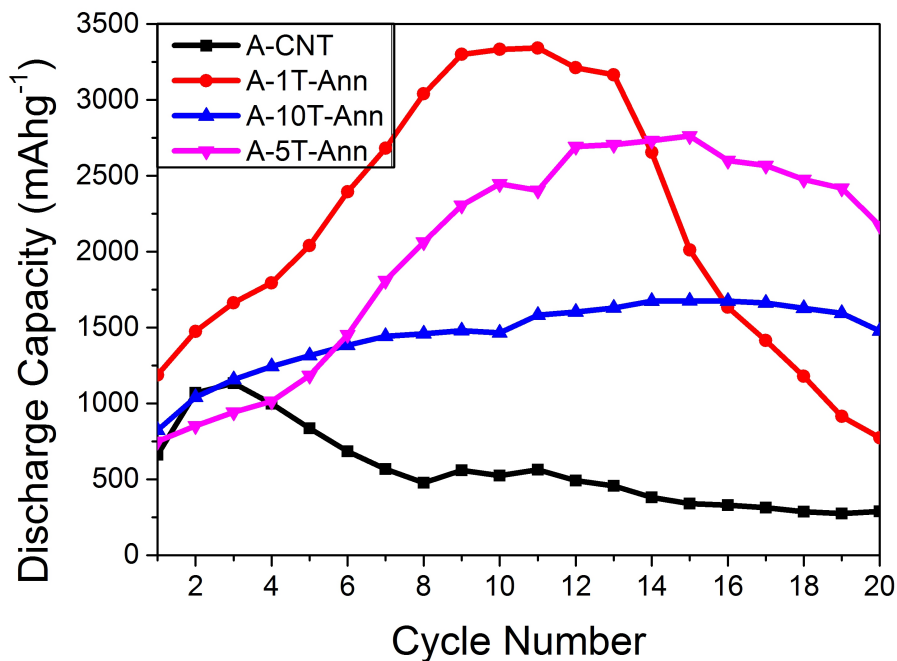


Figure 3.18: Discharge capacity retention comparison of A-10T-Ann, A-5T-Ann, A-1T-Ann and A-CNT cathodes on full 20 discharge and charge battery cycles at  $100 \text{ mA g}^{-1}$  current rate.

A-1T-Ann cathodes and acid functionalized CNT (A-CNT) are given. As can be seen from the figure, uniform and ultrathin  $\text{TiO}_2$  coatings were obtained on A-10T-Ann and A-5T-Ann cathodes. Effective  $\text{TiO}_2$  thicknesses on these samples were below a single nanometer, corresponding to less than a few monolayers. It is important to note that since the coating is ultra thin, it is extremely challenging to obtain a uniform coating alongside the high-surface area CNT walls. Nevertheless, high-resolution TEM analysis confirmed that we were able to obtain uniform, conformal, and sub-nm  $\text{TiO}_2$  coatings with the help of effective acid functionalization of the CNTs surface (Figure 3.17). However for A-1T-Ann cathode,  $\text{TiO}_2$  coating almost did not happen. If the TEM images of A-1T-Ann and A-CNT are compared, it can be seen that CNT surfaces of both cathode are bare. This is in fact understandable since one ALD cycle is correspond to one monolayer amount of precursor and it is almost impossible to actively coat all the CNT surface with such a less amount.

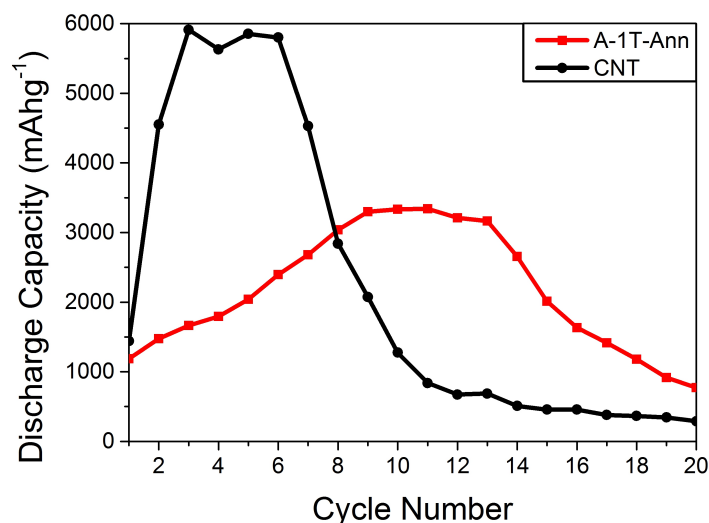


Figure 3.19: Discharge capacity retention comparison of A-1T-Ann and CNT cathodes on full 20 discharge and charge battery cycles at  $100 \text{ mA g}^{-1}$  current rate.

In Figure 3.18, a comparison of battery performances of A-10T-Ann, A-5T-Ann, A-1T-Ann and A-CNT are given. The cathodes were subjected to 20 full discharge and charge cycles at  $100 \text{ mA g}^{-1}$  current rate. At the first cycle A-10T-Ann, A-5T-Ann and A-CNT cathodes showed very similar capacities however on the following cycles while A-CNT cathode was losing its capacity, A-10T-Ann and A-5T-Ann cathodes showed excellent capacity retention with higher capacities. A-1T-Ann on the other hand showed a strange capacity retention behavior. Even though the capacity of A-1T-Ann cathode increased extremely until the 10<sup>th</sup> cycle, it drop down dramatically on the following cycles. Since A-1T-Ann cathode does not really have a  $\text{TiO}_2$  coating, the first thing come to mind was it might show the behavior of a A-CNT cathode. However A-CNT cathode showed a rather different capacity retention behavior and also a much lower capacity. Having considering A-1T-Ann cathode was went through an annealing process, the functional groups on the surface of the CNTs were most likely be deactivated and for this reason it is thought that A-1T-Ann cathode might show a similar capacity retention behavior to bare CNT cathode. At this point a bare CNT cathode was decided to be tested for battery performance in order to compare it with A-1T-Ann cathode and also the coated cathode

for an overall comparison. As shown in the Figure 3.19, the capacity retention behavior of A-1T-Ann and bare CNT cathodes are quite similar in terms of capacity increase in the first cycles following by a dramatic drop in the further cycles. CNT cathode however reached much larger capacity values because of lower weight and higher overall surface area for discharge products to grow on since functionalization, TiO<sub>2</sub> coating and annealing processes probably result in some entanglement, pore clogging and as a result lower surface area.

### 3.3 Stability Tests of Li-O<sub>2</sub> Battery Cathode

After many trial on surface modification techniques and optimization studies on TiO<sub>2</sub> coating by ALD, annealed acid functionalized CNT with 5 ALD cycles TiO<sub>2</sub> coating (A-5T-Ann) was chosen to be the ultimate cathode recipe for a stable cathode for Li-O<sub>2</sub> batteries in this study. In this section the electrochemical and battery performances along with cathode stability of A-5T-Ann cathode will be investigated and compared with non-coated CNT cathodes.

In order to compare the electrochemical activity of CNT and 5T cathodes, cyclic voltammetry (CV) analyses were performed for each cathodes. (Figure 3.20) Cathodic and anodic peaks for each electrodes represent reversible electrochemical reactions. Peaks at  $\sim 2.55$  V and  $\sim 3.25$  V represent Li<sub>2</sub>O<sub>2</sub> formation and decomposition, respectively for both electrodes. The electrodes were both subjected to two CV cycles.

On Li<sub>2</sub>O<sub>2</sub> formation peak, both electrodes showed an increase in the potential on the second CV cycle, which might be related to a possible surface activation upon cycling. On the other hand, while Li<sub>2</sub>O<sub>2</sub> decomposition peaks on the first and the second CV cycles for 5T electrode are in the same potential, the first peak for CNT electrode is shifted from 3.23 V to 3.29 V on the second CV cycle. The increase in the potential of second CV cycle indicates that overpotential was increasing upon cycling, which was probably due to side product formation on CNT cathode surface.

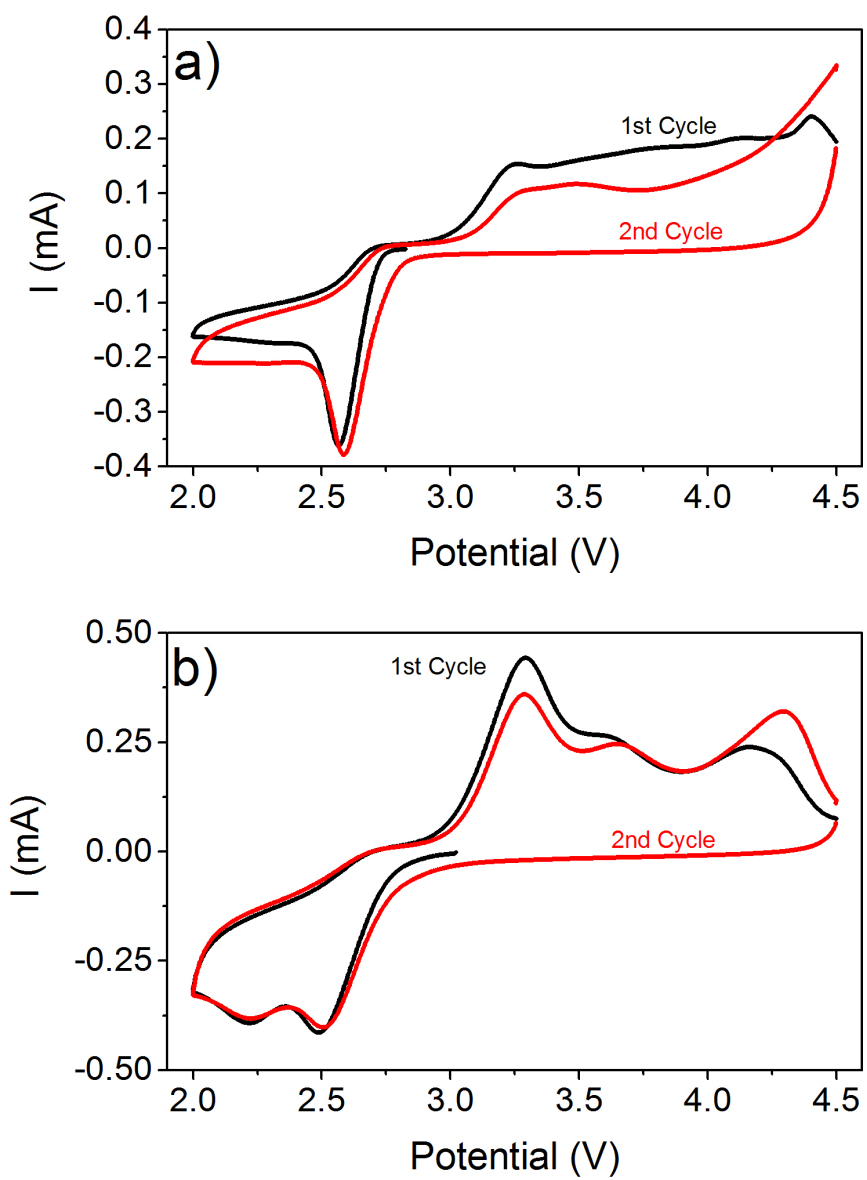


Figure 3.20: CV curves of a) CNT, b) A-5T-Ann electrodes

In Figure 3.21, full capacity discharge and charge curves of 1<sup>st</sup>, 5<sup>th</sup>, 10<sup>th</sup> and 20<sup>th</sup> battery cycles of CNT (Figure 3.21a)) and A-5T-Ann (Figure 3.21b)) are presented. Considering A-5T-Ann and first few cycles of CNT cathodes, discharge curves have a single and horizontal plateau around 2.7 V until reaching full capacity, which indicates a well-established discharge reaction. Charge curves showed several different plateaus until reaching the cut-off potential. This was explained by heterogeneous structural properties of the cathode [48] or disintegration of different Li<sub>2</sub>O<sub>2</sub> morphologies in different sizes during charge [103] in some previous studies.

Since battery cells were subjected to full-capacity cycles, it is rather expected to observe slightly different capacities as cycling proceeds as mentioned before. Nevertheless there is one critical point to discuss. Interestingly, all cathodes showed a fairly significant capacity increase in the first few cycles on full capacity battery cycling. Such capacity increase was also observed in some previous studies. [104, 105] Meini et al. [106] attributed this behavior to the differentiation of electrolyte composition with its decomposition at high potentials. This explanation is coherent with our observations since electrolyte decomposition is evidenced as further discussed below. On the other hand, as an educated guess, this behavior might be related to a possible surface activation of the relevant cathode upon cycling until reaching the real capacity value of the cathode. This is not actually a proved idea since there is not much published research studies that working with full capacity battery cycling of Li-O<sub>2</sub> batteries, however having experiencing this behavior on all the cathodes, it might actually be the reason.

Non-coated CNT cathode showed a relatively high discharge capacity at the first few cycles, which is consistent with its naturally high gravimetric energy density, but dropped dramatically in subsequent cycles and finally lost more than 90% of its original capacity at the 20<sup>th</sup> cycle. Similarly, A-CNT cathode, which is the base material of TiO<sub>2</sub> coated cathodes, showed relatively low discharge capacity and similar to bare CNT cathode, very poor capacity retention (Figure 3.18). We relate the low capacity observed in A-CNT cathode to unused interior surfaces and pores due to accumulation of the discharge products, Li<sub>2</sub>O<sub>2</sub>, only on the outermost surface. This can be a result of strong interaction of functional

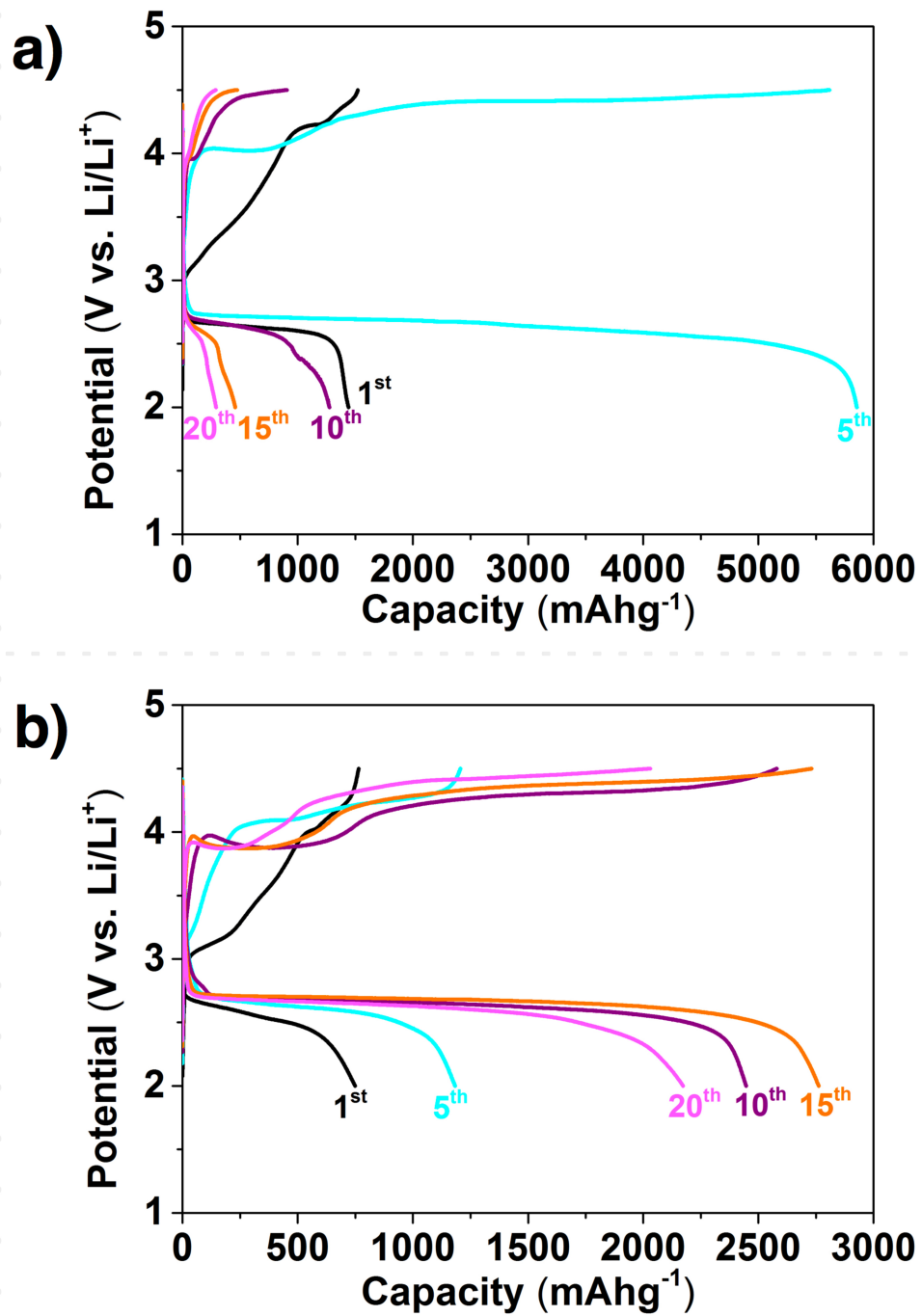


Figure 3.21: Full capacity discharge and charge curves of a) CNT, b) A-5T-Ann cathodes.

groups presented on A-CNT's surface with  $\text{Li}^+$  ions and  $\text{O}_2$  molecules, which might trigger the  $\text{Li}_2\text{O}_2$  formation before they could diffuse into interior surfaces and pores.

The poor capacity retention of the non-coated CNT and A-CNT cathodes is attributed to the cathode degradation upon battery cycling as discussed earlier. On the other hand, ALD-grown  $\text{TiO}_2$  coated cathodes showed excellent capacity retention behavior compared to non-coated counterparts. Among these results A-5T-Ann, which had the thinnest  $\text{TiO}_2$  coating deposited on CNTs, showed the best performance, reaching a capacity up to  $2700 \text{ mAhg}^{-1}$  even on its 15<sup>th</sup> cycle (Figure 3.18), while featuring an excellent capacity retention. On the other hand, A-20T-Ann and A-50T-Ann cathodes coated with  $\text{TiO}_2$  layers thicker than a few nanometers showed rather low capacities even if the capacity retentions were close-to perfect (Figure 3.18).

All the cycling tests were performed with the full capacity of the battery cells in order to demonstrate the actual stability of ultrathin  $\text{TiO}_2$  coatings employed in this study. While the full capacity of the non-coated pristine CNTs may appear to be larger compared to coated CNTs in the beginning, the poor retention of non-coated CNTs make this high initial capacity useless in a realistic system. This initially lower gravimetric capacity of coated cathodes compared to non-coated CNT can be explained by comparatively higher cathode weight of coated cathodes. Furthermore it should also be considered that low capacity A-CNT was used as a base material for  $\text{TiO}_2$  coating and the capacity of A-CNT cathodes actually increases after  $\text{TiO}_2$  coating.

Figure 3.22 shows the Nyquist plot of CNT and A-5T-Ann electrodes before and after CV measurement, which conducted at open circuit potential (OCV). Diameters of semicircles in the high frequency region indicate the resistance of the electrodes. The resistances coming from the battery cells are same for each electrodes. As expected, the diameter of semicircle is higher in A-5T-Ann compared to CNT electrode, which indicates electrode resistance is higher in A-5T-Ann. This is actually the reason why CNT cathode shows higher battery capacity compared to A-5T-Ann. However, after CV measurement, the diameter of the

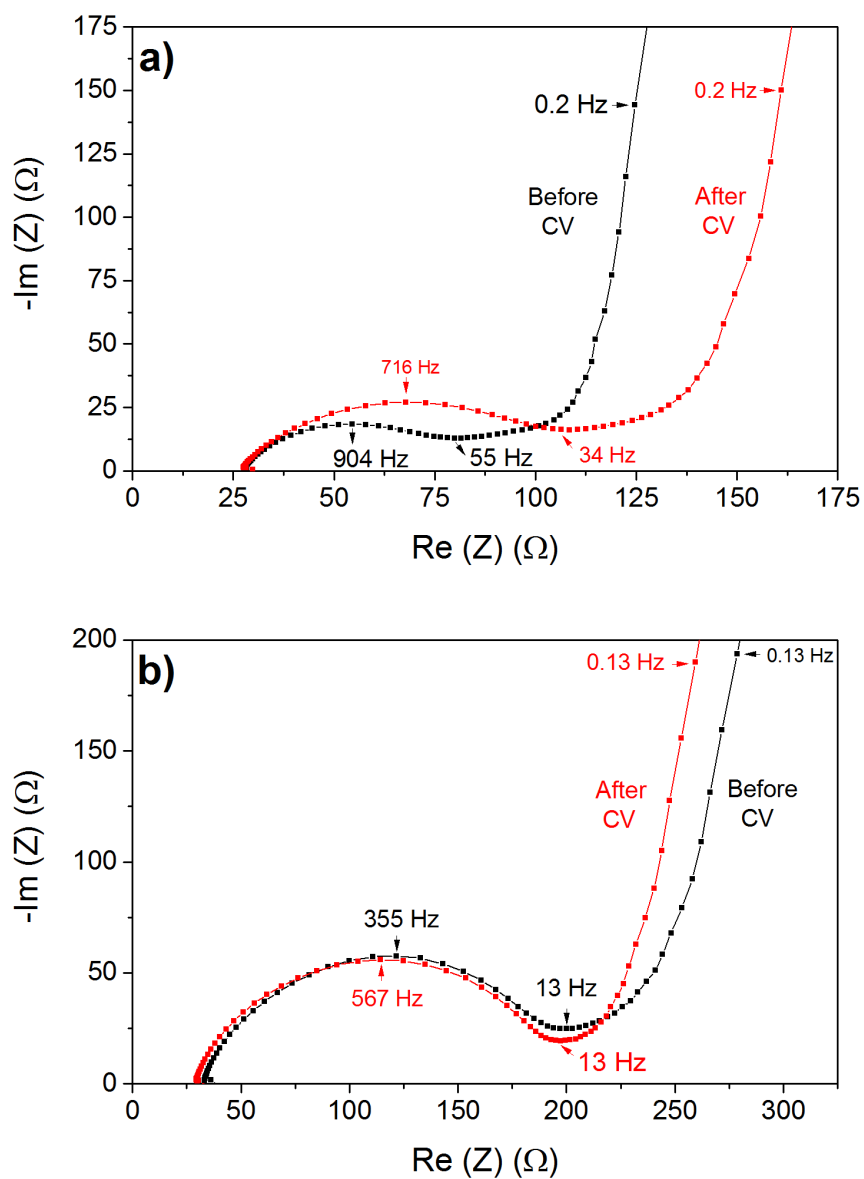


Figure 3.22: Nyquist plots of the impedance measurements of a) CNT, b) A-5T-Ann electrodes. OCV values for CNT electrode before and after CV are 2.786 V and 3.364 V respectively, and for A-5T-Ann electrode before and after CV are 3.116 V and 3.393 V, respectively.

semicircle is increased dramatically for CNT electrode after CV cycling while it remains the same for A-5T-Ann electrode. This was most probably because of the side product formation on CNT electrode surface after cycling, which decreased the electrical conductivity.

XPS analysis of pristine, meaning as prepared, and battery cycled cathodes was performed in order to assess the stability of TiO<sub>2</sub> coated and non-coated CNT cathodes. C1s and O1s XPS spectra of before and after battery cycling of A-5T-Ann and CNT cathodes are shown in Figure 3.23a and b). Considering C1s spectra, before battery cycling, C=C sp<sup>2</sup>, C-C sp<sup>3</sup>, and C-O peaks at 284.8, 285.3, and 287.3 eV binding energies respectively, can be observed for both cathodes. [107, 108] After 20 full capacity battery cycles, which were finished on charging state in the last cycle, carbonate peak (O=C-O) at 289.8 eV, which is the sign of side product Li<sub>2</sub>CO<sub>3</sub>, is visible in addition to other peaks. For A-5T-Ann cathode, C=C/C-C peaks still have the highest and almost same intensity and carbonate peak has comparatively much lower intensity after 20 full capacity battery cycles. On the other hand, for CNT cathode, carbonate and C-O peaks have the highest intensities after 20<sup>th</sup> charge and C=C/C-C peaks were diminished, which confirms that side products were dominating and covered the surface of CNT cathode. Additionally, a peak corresponding to CF<sub>2</sub> at 292 eV [109] is also detected, which is most probably related to electrolyte decomposition.

In O1s spectra of the A-5T-Ann cathode, the peaks corresponding to Ti-O bonds [107] exhibit the same intensity before and after battery cycling, which indicates the endurance of the TiO<sub>2</sub> coated cathode. The increased carbonate and C-O peaks intensities are most probably related to electrolyte decomposition in addition to unhindered cathode degradation. However for CNT, electrolyte decomposition related C-O and cathode degradation related carbonate peaks arise abruptly after 20<sup>th</sup> charge. It can also be seen from Figure 3.24 that, Li1s spectra of A-5T-Ann and CNT cathodes after 20 full capacity battery cycling, there is comparatively much more lithium product left on CNT surface than on A-5T-Ann cathode surface at the end of 20 cycles considering the broad range of lithium peaks. It is critical to emphasize again that a certain amount of electrolyte degradation was happening due to high voltages, which appears as an increase in

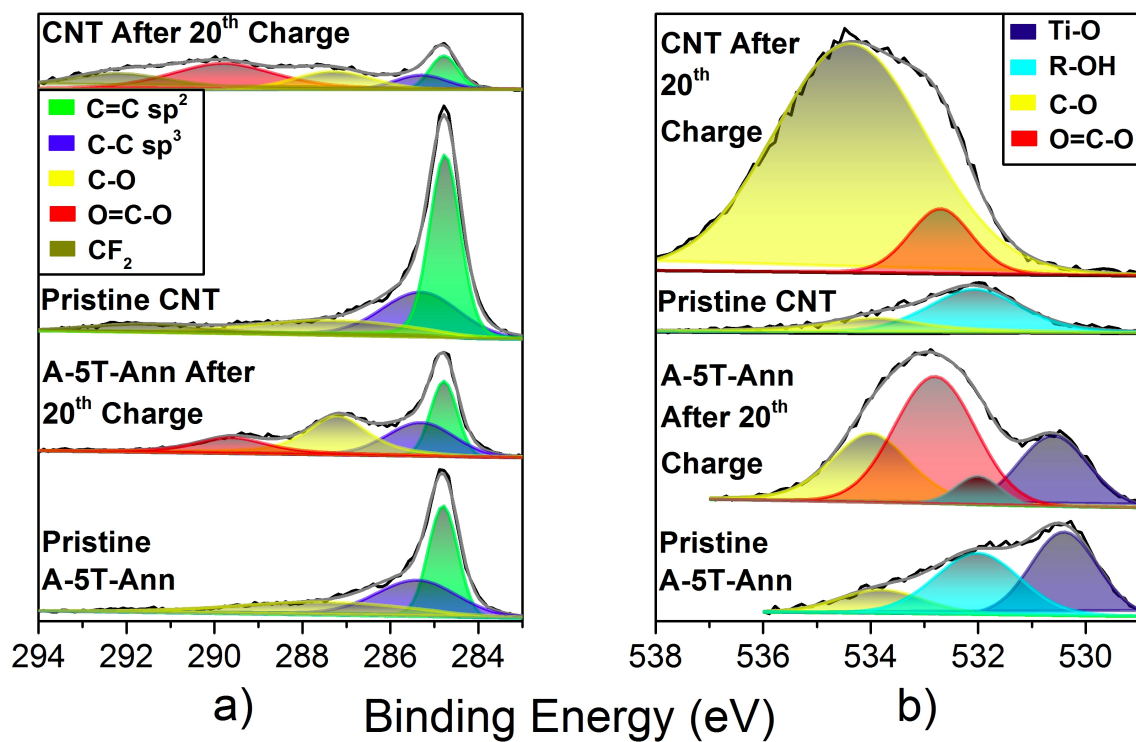


Figure 3.23: a) C1s and b) O1s XPS spectra of CNT and A-5T-Ann cathodes in their pristine state and after cycling at the end of 20<sup>th</sup> charge.

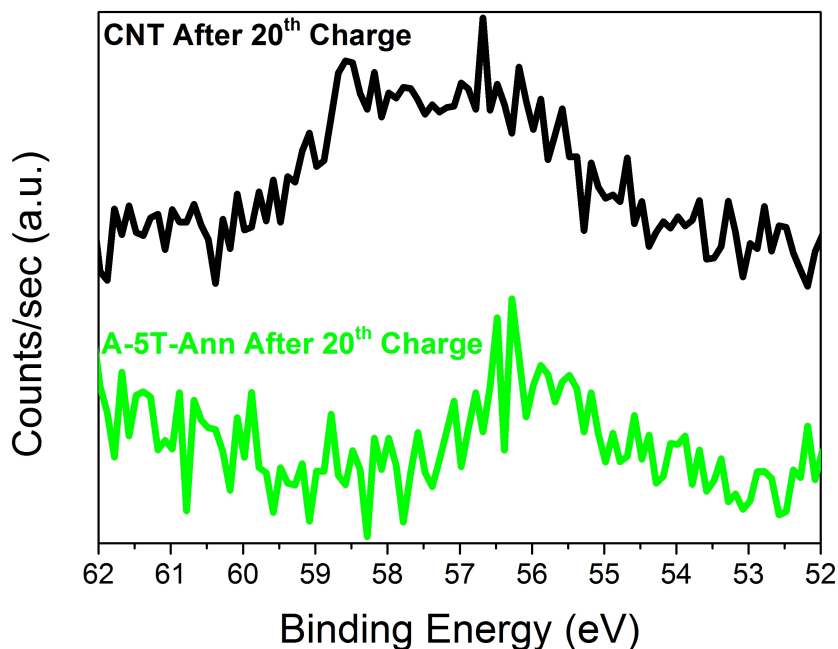


Figure 3.24: Li1s XPS spectra of CNT and A-5T-Ann cathodes after full capacity battery cycling at the end of 20<sup>th</sup> charge.

carbonate, C-O and corresponding lithium peaks for A-5T-Ann cathode after 20 full-capacity cycling.

These XPS results prove that; conformal and ultrathin TiO<sub>2</sub> indeed works as an effective protective layer, which substantially reduces the carbon cathode degradation upon battery cycling.

Finally, SEM imaging of pristine and cycled cathodes were carried out to further prove the stability of A-5T-Ann cathode. In Figure 3.25, SEM images of A-5T-Ann and CNT cathode surfaces before and after battery cycling are presented. While ALD TiO<sub>2</sub> coated CNTs are still clearly visible and almost did not change at all after 20<sup>th</sup> charge for A-5T-Ann cathode, CNTs on CNT cathode are completely buried by side products. This observation clearly visualizes the reason for dramatic capacity fading of CNT cathode upon battery cycling while showing the effect of protective conformal ALD coatings, even at the sub-nm scale.

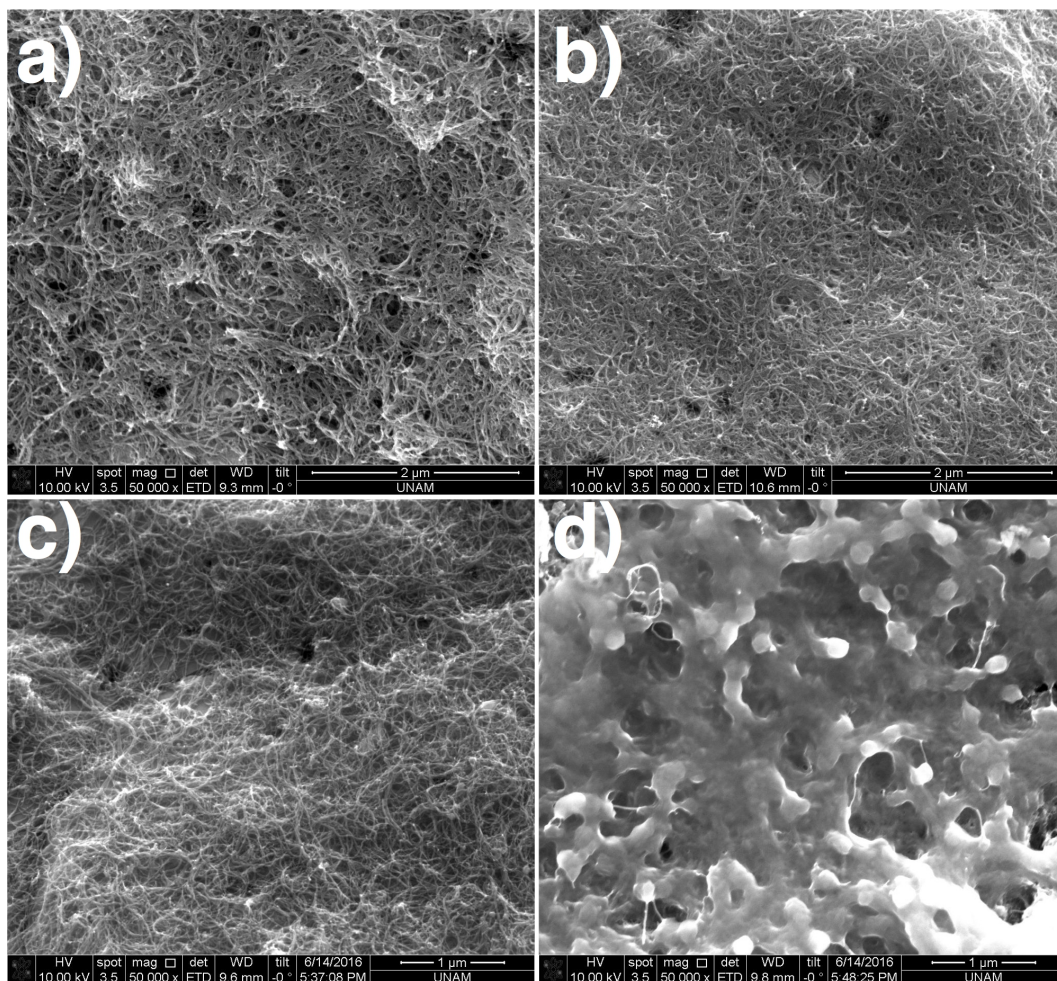


Figure 3.25: SEM images of a, b) A-5T-Ann and c, d) CNT cathodes in their a, c) pristine state and b, d) after cycling at the end of 20<sup>th</sup> charge.

# Chapter 4

## Conclusions

Energy demand is an essential issue in human life since the very beginning of the human history. It would not be an exaggeration to say that people need energy in every part of their life to live. In the early times it was only necessary for very basic needs like getting warm and nourishment but as the time passed it varied exponentially. In the modern times energy is necessary for almost every aspects of human life such as illumination, transportation, communication, entertainment etc. along with the very basic needs, like the old times. By the development of technology, energy demand is expanding with an increasing rate and becoming a more pronounced issue day by day.

Transportation forms a large part of the energy demand since the invention of motor vehicles and fossil fuels are the main energy source almost since the beginning. The popularity of fossil fuels as an energy source did not diminish for many years because of their high abundance, very easy and straightforward working mechanism and high energy efficiency. However using fossil fuels has its own drawbacks. First of all, fossil fuels are not very abundant anymore considering the increase amount of usage and exhausting natural sources. Secondly fossil fuel consumption is resulting into release of environmentally harmful greenhouse gasses that causes the global warming. These downsides push researchers to find alternatives to fossil fuels for using in transportation. Environmentally friendly,

high energy containing and limitless renewable energy sources like solar, tidal, wind, hydro or geothermal provide a perfect solution to this problem. However, these renewable energy sources are highly irregular, which means they either bound to a specific place or a specific time. In order to be able to use renewable energy sources in transportation, the extracted energy have to be stored. That is why energy storage plays a very important part in this issue.

An efficient energy storage system for transportation necessitates some vital features; low weight, high energy density and mobility. Among the energy storage systems the most suiting one for these features is batteries. In fact batteries are already being used in vehicles for providing small scale of energy. However, current commercially available batteries lack the sufficient energy density to be used as a propulsion unit in vehicles. On the contrary, there is one promising candidate that can possibly replace fossil fuels, which is Li-O<sub>2</sub> batteries.

Li-O<sub>2</sub> batteries are very promising candidates of energy storage systems for electric vehicles, thanks to their exceptionally high gravimetric energy density, which is approximately four times higher than state of art Li-ion batteries. There are two main reasons that make Li-O<sub>2</sub> batteries superior to Li-ion batteries. The first reason originates from the lightweight of the active cathode material that is used in Li-O<sub>2</sub> batteries, which is oxygen. This is actually the most distinctive feature of all metal air batteries. The second reason is the energy capacity of Li-O<sub>2</sub> batteries is not limited by the intercalation mechanism like Li-ion batteries rather it has extensive reaction sites for discharge products to form. Nevertheless, Li-O<sub>2</sub> batteries suffer from some major problems that need to be overcome in order to be commercially realized. These problems are centered around unstable cathode and electrolyte materials. In this thesis study, unstable cathode material problem for Li-O<sub>2</sub> batteries tried to be addressed and thankfully very promising results were obtained.

Li-O<sub>2</sub> batteries consist of three main compartments; a lithium anode, an ionically conductive but electrically insulative electrolyte material and one electrically conductive, high surface area cathode material. The main working mechanism of Li-O<sub>2</sub> batteries is like the following: On discharge Li<sup>+</sup> ions from lithium metal go

through to electrolyte and react with  $O_2$  molecules and reduce to form the main discharge product,  $Li_2O_2$ , on the cathode surface and generate electricity. On charge, the discharge product,  $Li_2O_2$ , disintegrate to  $Li^+$  ions and  $O_2$  molecules with an external energy supply.

In Li- $O_2$  batteries carbon based materials are frequently used as a cathode material because of its exceptional properties like high surface area, high porosity, high electrical conductivity and lightweight. However carbon based materials are not stable upon cycling in Li- $O_2$  battery environment. The instability arises especially on cathode electrolyte interface at high voltages. The formed  $Li_2O_2$  is reacting with carbon to form unwanted side products like  $Li_2CO_3$ , which accumulate on the cathode surface and result into capacity fading upon battery cycling.

The motivation of this study is to take the advantages of the carbon based materials as a cathode material for Li- $O_2$  batteries while preventing it from degradation by producing a stable carbon based cathode material. In order to do this, an ultra thin and uniform layer of  $TiO_2$  is coated by atomic layer deposition method to CNT surface to prevent unwanted interactions on cathode electrolyte interface in battery operations while allowing the main battery reactions to happen.

ALD necessitates a hydrophilic surface with functional groups attached to it. However CNTs have a hydrophobic surface so in order to be able to coat CNTs surface with  $TiO_2$  by ALD, a prior surface modification process to the CNTs need to be performed. Three different surface modification processes were performed in this study; plasma ashing, CTAB and acid functionalization. Among this three, the most successful and reliable surface modification method was acid functionalization. After this process the next step was the optimization of  $TiO_2$  coating. Several ALD cycles had been tried; from 100 cycles to 1 cycle, in order to find out the optimum ALD cycles for coating. TEM imaging and battery tests were performed to each coated cathode simultaneously. Battery tests were performed under full capacity discharge and charge cycles to be able to produce a cathode that is stable under the conditions as near as possible to the commercialized battery systems. After several characterization tests and discussions, 5

ALD cycles TiO<sub>2</sub> coated and annealed cathode (A-5T-Ann) was found out to be the best coating recipe for a stable Li-O<sub>2</sub> batteries in this study. Additional cyclic voltammetry and impedance spectroscopy measurement results were also showing the enhanced stability of TiO<sub>2</sub> coated CNTs compared to bare CNTs.

In order to prove the stability of this cathode XPS characterization and SEM imaging were performed. XPS characterization results revealed that TiO<sub>2</sub> coating on CNT dramatically reduces the side product formation upon battery cycling compared to bare CNT cathodes. A-5T-Ann cathode showed excellent stability and capacity retention after 20 full discharge and charge battery cycles. On the other hand, the capacity of CNT dropped almost 90% after 20 battery cycles. SEM images also revealed that the surface of CNT cathode was completely covered with side products after 20 battery cycles while it was almost completely unchanged for A-5T-Ann cathode.

# Bibliography

- [1] U. S. Briefing, “International energy outlook 2013,” *US Energy Information Administration*, 2013.
- [2] I. P. on Climate Change, *Climate change 2014: mitigation of climate change*, vol. 3. Cambridge University Press, 2015.
- [3] V. Arunachalam and E. Fleischer, “The global energy landscape and materials innovation,” *MRS bulletin*, vol. 33, no. 04, pp. 264–288, 2008.
- [4] Y. Wang, Z. Shi, Y. Huang, Y. Ma, C. Wang, M. Chen, and Y. Chen, “Supercapacitor devices based on graphene materials,” *The Journal of Physical Chemistry C*, vol. 113, no. 30, pp. 13103–13107, 2009.
- [5] B. E. Conway, “Transition from supercapacitor to battery behavior in electrochemical energy storage,” *Journal of the Electrochemical Society*, vol. 138, no. 6, pp. 1539–1548, 1991.
- [6] J. R. Miller and A. F. Burke, “Electrochemical capacitors: challenges and opportunities for real-world applications,” *The Electrochemical Society Interface*, vol. 17, no. 1, p. 53, 2008.
- [7] L. L. Zhang and X. Zhao, “Carbon-based materials as supercapacitor electrodes,” *Chemical Society Reviews*, vol. 38, no. 9, pp. 2520–2531, 2009.
- [8] P. Simon and Y. Gogotsi, “Materials for electrochemical capacitors,” *Nature materials*, vol. 7, no. 11, pp. 845–854, 2008.
- [9] O. Haas and E. J. Cairns, “Electrochemical energy storage,” *Annual Reports Section C (Physical Chemistry)*, vol. 95, pp. 163–198, 1999.

- [10] A. Boulabiar, K. Bouraoui, M. Chastrette, and M. Abderrabba, "A historical analysis of the Daniell cell and electrochemistry teaching in French and Tunisian textbooks," *J. Chem. Educ.*, vol. 81, no. 5, p. 754, 2004.
- [11] M. Armand and J.-M. Tarascon, "Building better batteries," *Nature*, vol. 451, no. 7179, pp. 652–657, 2008.
- [12] H. Bode, "Lead-acid batteries," *Wiley*, 1977.
- [13] D. Linden and T. B. Reddy, "Handbook of batteries. 3rd," 2002.
- [14] A. Taniguchi, N. Fujioka, M. Ikoma, and A. Ohta, "Development of nickel/metal-hydride batteries for EVs and HEVs," *Journal of Power Sources*, vol. 100, no. 1, pp. 117–124, 2001.
- [15] J.-P. Gabano, "Lithium batteries," *London and New York, Academic Press, 1983, 467 p.*, vol. 1, 1983.
- [16] H. Takeshita, "Portable Li-ion, worldwide," in *Proc. Conf. Power*, 2000.
- [17] W. Van Gool, *Fast ion transport in solids, solid state batteries and devices. (Proceedings of the NATO-sponsored advanced study institute of fast ion transport in solids, solid state batteries and devices, Belgrade, Italy 5-15 September 1972)*. Elsevier, New York, 1973.
- [18] M. S. Whittingham, "Electrical energy storage and intercalation chemistry," *Science*, vol. 192, no. 4244, pp. 1126–1127, 1976.
- [19] P. Voelker, "Trace degradation analysis of lithium-ion battery components," *R&D Magazine*, 2014.
- [20] D. Murphy and P. Christian, "Solid state electrodes for high energy batteries," *Science*, vol. 205, no. 4407, pp. 651–656, 1979.
- [21] K. Mizushima, P. Jones, P. Wiseman, and J. Goodenough, "LiCoO<sub>2</sub> (01x1): A new cathode material for batteries of high energy density," *Materials Research Bulletin*, vol. 15, no. 6, pp. 783–789, 1980.

- [22] M. Thackeray, W. David, P. Bruce, and J. Goodenough, “Lithium insertion into manganese spinels,” *Materials Research Bulletin*, vol. 18, no. 4, pp. 461–472, 1983.
- [23] D. Murphy, F. Di Salvo, J. Carides, and J. Waszczak, “Topochemical reactions of rutile related structures with lithium,” *Materials Research Bulletin*, vol. 13, no. 12, pp. 1395–1402, 1978.
- [24] T. Nagaura and K. Tozawa, “Lithium ion rechargeable battery,” *Prog. Batteries Solar Cells*, vol. 9, p. 209, 1990.
- [25] J.-M. Tarascon and M. Armand, “Issues and challenges facing rechargeable lithium batteries,” *Nature*, vol. 414, no. 6861, pp. 359–367, 2001.
- [26] Wikipedia, “Rechargeable battery — wikipedia, the free encyclopedia,” 2016. [Online; accessed 15-August-2016].
- [27] Z. Yang, J. Zhang, M. C. Kintner-Meyer, X. Lu, D. Choi, J. P. Lemmon, and J. Liu, “Electrochemical energy storage for green grid,” *Chemical reviews*, vol. 111, no. 5, pp. 3577–3613, 2011.
- [28] S. Yuvaraj, R. K. Selvan, and Y. S. Lee, “An overview of ab 2 o 4-and a 2 bo 4-structured negative electrodes for advanced li-ion batteries,” *RSC Advances*, vol. 6, no. 26, pp. 21448–21474, 2016.
- [29] I. E. Commission, “White papers: Electrical energy storage,” *International Electrotechnical Commission. IEC*, 2011.
- [30] B. Scrosati and J. Garche, “Lithium batteries: Status, prospects and future,” *Journal of Power Sources*, vol. 195, no. 9, pp. 2419–2430, 2010.
- [31] M. Obrovac and L. Christensen, “Structural changes in silicon anodes during lithium insertion/extraction,” *Electrochemical and Solid-State Letters*, vol. 7, no. 5, pp. A93–A96, 2004.
- [32] C. K. Chan, H. Peng, G. Liu, K. McIlwrath, X. F. Zhang, R. A. Huggins, and Y. Cui, “High-performance lithium battery anodes using silicon nanowires,” *Nature nanotechnology*, vol. 3, no. 1, pp. 31–35, 2008.

- [33] U. Kasavajjula, C. Wang, and A. J. Appleby, "Nano-and bulk-silicon-based insertion anodes for lithium-ion secondary cells," *Journal of Power Sources*, vol. 163, no. 2, pp. 1003–1039, 2007.
- [34] J.-G. Zhang, D. Wang, W. Xu, J. Xiao, and R. E. Williford, "Ambient operation of li/air batteries," *Journal of Power Sources*, vol. 195, no. 13, pp. 4332–4337, 2010.
- [35] D. Zhang, R. Li, T. Huang, and A. Yu, "Novel composite polymer electrolyte for lithium air batteries," *Journal of Power Sources*, vol. 195, no. 4, pp. 1202–1206, 2010.
- [36] G. Girishkumar, B. McCloskey, A. Luntz, S. Swanson, and W. Wilcke, "Lithium- air battery: promise and challenges," *The Journal of Physical Chemistry Letters*, vol. 1, no. 14, pp. 2193–2203, 2010.
- [37] E. L. Littauer and K. C. Tsai, "Anodic behavior of lithium in aqueous electrolytes i. transient passivation," *Journal of the Electrochemical Society*, vol. 123, no. 6, pp. 771–776, 1976.
- [38] K. Abraham and Z. Jiang, "A polymer electrolyte-based rechargeable lithium/oxygen battery," *Journal of The Electrochemical Society*, vol. 143, no. 1, pp. 1–5, 1996.
- [39] P. G. Bruce, S. A. Freunberger, L. J. Hardwick, and J.-M. Tarascon, "Li-o<sub>2</sub> and li-s batteries with high energy storage," *Nature materials*, vol. 11, no. 1, pp. 19–29, 2012.
- [40] J. Lu, L. Li, J.-B. Park, Y.-K. Sun, F. Wu, and K. Amine, "Aprotic and aqueous li-o<sub>2</sub> batteries," *Chemical reviews*, vol. 114, no. 11, pp. 5611–5640, 2014.
- [41] N. Garcia-Araez and P. Novák, "Critical aspects in the development of lithium–air batteries," *Journal of Solid State Electrochemistry*, vol. 17, no. 7, pp. 1793–1807, 2013.

- [42] J.-G. Zhang, D. Wang, W. Xu, J. Xiao, and R. E. Williford, "Ambient operation of li/air batteries," *Journal of Power Sources*, vol. 195, no. 13, pp. 4332–4337, 2010.
- [43] J. Read, K. Mutolo, M. Ervin, W. Behl, J. Wolfenstine, A. Driedger, and D. Foster, "Oxygen transport properties of organic electrolytes and performance of lithium/oxygen battery," *Journal of The Electrochemical Society*, vol. 150, no. 10, pp. A1351–A1356, 2003.
- [44] W. Xu, J. Xiao, J. Zhang, D. Wang, and J.-G. Zhang, "Optimization of nonaqueous electrolytes for primary lithium/air batteries operated in ambient environment," *Journal of the Electrochemical Society*, vol. 156, no. 10, pp. A773–A779, 2009.
- [45] J. Xiao, W. Xu, D. Wang, and J.-G. Zhang, "Hybrid air-electrode for li/air batteries," *Journal of The Electrochemical Society*, vol. 157, no. 3, pp. A294–A297, 2010.
- [46] J. Christensen, P. Albertus, R. S. Sanchez-Carrera, T. Lohmann, B. Kozinsky, R. Liedtke, J. Ahmed, and A. Kojic, "A critical review of li/air batteries," *Journal of the Electrochemical Society*, vol. 159, no. 2, pp. R1–R30, 2011.
- [47] R. R. Mitchell, B. M. Gallant, C. V. Thompson, and Y. Shao-Horn, "All-carbon-nanofiber electrodes for high-energy rechargeable li-o<sub>2</sub> batteries," *Energy & Environmental Science*, vol. 4, no. 8, pp. 2952–2958, 2011.
- [48] M. M. Ottakam Thotiyl, S. A. Freunberger, Z. Peng, and P. G. Bruce, "The carbon electrode in nonaqueous li-o<sub>2</sub> cells," *Journal of the American Chemical Society*, vol. 135, no. 1, pp. 494–500, 2012.
- [49] J. Lu, Y. Lei, K. C. Lau, X. Luo, P. Du, J. Wen, R. S. Assary, U. Das, D. J. Miller, J. W. Elam, *et al.*, "A nanostructured cathode architecture for low charge overpotential in lithium-oxygen batteries," *Nature communications*, vol. 4, 2013.

- [50] Z.-L. Wang, D. Xu, J.-J. Xu, L.-L. Zhang, and X.-B. Zhang, “Graphene oxide gel-derived, free-standing, hierarchically porous carbon for high-capacity and high-rate rechargeable li-o<sub>2</sub> batteries,” *Advanced Functional Materials*, vol. 22, no. 17, pp. 3699–3705, 2012.
- [51] Q. Li, R. Cao, J. Cho, and G. Wu, “Nanostructured carbon-based cathode catalysts for nonaqueous lithium–oxygen batteries,” *Physical Chemistry Chemical Physics*, vol. 16, no. 27, pp. 13568–13582, 2014.
- [52] Y. Zhang, H. Zhang, J. Li, M. Wang, H. Nie, and F. Zhang, “The use of mixed carbon materials with improved oxygen transport in a lithium-air battery,” *Journal of Power Sources*, vol. 240, pp. 390–396, 2013.
- [53] K.-H. Xue, T.-K. Nguyen, and A. A. Franco, “Impact of the cathode microstructure on the discharge performance of lithium air batteries: a multiscale model,” *Journal of The Electrochemical Society*, vol. 161, no. 8, pp. E3028–E3035, 2014.
- [54] Y. Li, K. Guo, J. Li, X. Dong, T. Yuan, X. Li, and H. Yang, “Controllable synthesis of ordered mesoporous nife<sub>2</sub>o<sub>4</sub> with tunable pore structure as a bifunctional catalyst for li–o<sub>2</sub> batteries,” *ACS applied materials & interfaces*, vol. 6, no. 23, pp. 20949–20957, 2014.
- [55] C. Xia, M. Waletzko, K. Pepller, and J. Janek, “Silica nanoparticles as structural promoters for oxygen cathodes of lithium–oxygen batteries,” *The Journal of Physical Chemistry C*, vol. 117, no. 39, pp. 19897–19904, 2013.
- [56] S. A. Freunberger, Y. Chen, N. E. Drewett, L. J. Hardwick, F. Bardé, and P. G. Bruce, “The lithium–oxygen battery with ether-based electrolytes,” *Angewandte Chemie International Edition*, vol. 50, no. 37, pp. 8609–8613, 2011.
- [57] Y. Li, J. Wang, X. Li, J. Liu, D. Geng, J. Yang, R. Li, and X. Sun, “Nitrogen-doped carbon nanotubes as cathode for lithium–air batteries,” *Electrochemistry Communications*, vol. 13, no. 7, pp. 668–672, 2011.

- [58] G. Zhang, J. Zheng, R. Liang, C. Zhang, B. Wang, M. Hendrickson, and E. Plichta, "Lithium-air batteries using swnt/cnf buckypapers as air electrodes," *Journal of The Electrochemical Society*, vol. 157, no. 8, pp. A953–A956, 2010.
- [59] J. Li, N. Wang, Y. Zhao, Y. Ding, and L. Guan, "Mno<sub>2</sub> nanoflakes coated on multi-walled carbon nanotubes for rechargeable lithium-air batteries," *Electrochemistry Communications*, vol. 13, no. 7, pp. 698–700, 2011.
- [60] G. Zhang, J. Zheng, R. Liang, C. Zhang, B. Wang, M. Au, M. Hendrickson, and E. Plichta, " $\alpha$ -mno<sub>2</sub>/carbon nanotube/carbon nanofiber composite catalytic air electrodes for rechargeable lithium-air batteries," *Journal of The Electrochemical Society*, vol. 158, no. 7, pp. A822–A827, 2011.
- [61] G. Wu, N. H. Mack, W. Gao, S. Ma, R. Zhong, J. Han, J. K. Baldwin, and P. Zelenay, "Nitrogen-doped graphene-rich catalysts derived from heteroatom polymers for oxygen reduction in nonaqueous lithium-o<sub>2</sub> battery cathodes," *Acs Nano*, vol. 6, no. 11, pp. 9764–9776, 2012.
- [62] Q. Li, P. Xu, W. Gao, S. Ma, G. Zhang, R. Cao, J. Cho, H.-L. Wang, and G. Wu, "Graphene/graphene-tube nanocomposites templated from cage-containing metal-organic frameworks for oxygen reduction in li-o<sub>2</sub> batteries," *Advanced materials*, vol. 26, no. 9, pp. 1378–1386, 2014.
- [63] J. Xiao, D. Mei, X. Li, W. Xu, D. Wang, G. L. Graff, W. D. Bennett, Z. Nie, L. V. Saraf, I. A. Aksay, *et al.*, "Hierarchically porous graphene as a lithium-air battery electrode," *Nano letters*, vol. 11, no. 11, pp. 5071–5078, 2011.
- [64] J. Kim, J. Lee, and Y. Tak, "Relationship between carbon corrosion and positive electrode potential in a proton-exchange membrane fuel cell during start/stop operation," *Journal of Power Sources*, vol. 192, no. 2, pp. 674–678, 2009.
- [65] B. M. Gallant, R. R. Mitchell, D. G. Kwabi, J. Zhou, L. Zuin, C. V. Thompson, and Y. Shao-Horn, "Chemical and morphological changes of

- li-o<sub>2</sub> battery electrodes upon cycling,” *The Journal of Physical Chemistry C*, vol. 116, no. 39, pp. 20800–20805, 2012.
- [66] B. McCloskey, A. Speidel, R. Scheffler, D. Miller, V. Viswanathan, J. Hummelshøj, J. Nørskov, and A. Luntz, “Twin problems of interfacial carbonate formation in nonaqueous li-o<sub>2</sub> batteries,” *The journal of physical chemistry letters*, vol. 3, no. 8, pp. 997–1001, 2012.
- [67] A. Riaz, K.-N. Jung, W. Chang, S.-B. Lee, T.-H. Lim, S.-J. Park, R.-H. Song, S. Yoon, K.-H. Shin, and J.-W. Lee, “Carbon-free cobalt oxide cathodes with tunable nanoarchitectures for rechargeable lithium-oxygen batteries,” *Chemical Communications*, vol. 49, no. 53, pp. 5984–5986, 2013.
- [68] B. Wu, H. Zhang, W. Zhou, M. Wang, X. Li, and H. Zhang, “Carbon-free coo mesoporous nanowire array cathode for high-performance aprotic li-o<sub>2</sub> batteries,” *ACS Applied Materials & Interfaces*, vol. 7, no. 41, pp. 23182–23189, 2015.
- [69] G. Zhao, J. Lv, Z. Xu, L. Zhang, and K. Sun, “Carbon and binder free rechargeable li-o<sub>2</sub> battery cathode with pt/co<sub>3</sub>o<sub>4</sub> flake arrays as catalyst,” *Journal of Power Sources*, vol. 248, pp. 1270–1274, 2014.
- [70] F. Li, D.-M. Tang, Y. Chen, D. Golberg, H. Kitaura, T. Zhang, A. Yamada, and H. Zhou, “Ru/ito: a carbon-free cathode for nonaqueous li-o<sub>2</sub> battery,” *Nano letters*, vol. 13, no. 10, pp. 4702–4707, 2013.
- [71] F. Li, D.-M. Tang, Z. Jian, D. Liu, D. Golberg, A. Yamada, and H. Zhou, “Li-o<sub>2</sub> battery based on highly efficient sb-doped tin oxide supported ru nanoparticles,” *Advanced Materials*, vol. 26, no. 27, pp. 4659–4664, 2014.
- [72] K. Liao, T. Zhang, Y. Wang, F. Li, Z. Jian, H. Yu, and H. Zhou, “Nanoporous ru as a carbon-and binder-free cathode for li-o<sub>2</sub> batteries,” *ChemSusChem*, vol. 8, no. 8, pp. 1429–1434, 2015.
- [73] G. Zhao, R. Mo, B. Wang, L. Zhang, and K. Sun, “Enhanced cyclability of li-o<sub>2</sub> batteries based on tio<sub>2</sub> supported cathodes with no carbon or binder,” *Chemistry of Materials*, vol. 26, no. 8, pp. 2551–2556, 2014.

- [74] G. Zhao, Y. Niu, L. Zhang, and K. Sun, "Ruthenium oxide modified titanium dioxide nanotube arrays as carbon and binder free lithium-air battery cathode catalyst," *Journal of Power Sources*, vol. 270, pp. 386–390, 2014.
- [75] Z. Peng, S. A. Freunberger, Y. Chen, and P. G. Bruce, "A reversible and higher-rate li-o<sub>2</sub> battery," *Science*, vol. 337, no. 6094, pp. 563–566, 2012.
- [76] M. M. O. Thotiyl, S. A. Freunberger, Z. Peng, Y. Chen, Z. Liu, and P. G. Bruce, "A stable cathode for the aprotic li-o<sub>2</sub> battery," *Nature materials*, vol. 12, no. 11, pp. 1050–1056, 2013.
- [77] B. D. Adams, R. Black, C. Radtke, Z. Williams, B. L. Mehdi, N. D. Browning, and L. F. Nazar, "The importance of nanometric passivating films on cathodes for li-air batteries," *ACS nano*, vol. 8, no. 12, pp. 12483–12493, 2014.
- [78] H. Kim, W.-J. Maeng, *et al.*, "Applications of atomic layer deposition to nanofabrication and emerging nanodevices," *Thin Solid Films*, vol. 517, no. 8, pp. 2563–2580, 2009.
- [79] S. M. George, "Atomic layer deposition: an overview," *Chemical reviews*, vol. 110, no. 1, pp. 111–131, 2009.
- [80] M. Ritala and M. Leskela, "Atomic layer deposition," *Handbook of thin film materials*, vol. 1, pp. 103–159, 2001.
- [81] R. Lapshin, A. Alekhin, A. Kirilenko, S. Odintsov, and V. Krotkov, "Vacuum ultraviolet smoothing of nanometer-scale asperities of poly (methyl methacrylate) surface," *Journal of Surface Investigation. X-ray, Synchrotron and Neutron Techniques*, vol. 4, no. 1, pp. 1–11, 2010.
- [82] A. Alekhin, G. Boleiko, S. Gudkova, A. Markeev, A. Sigarev, V. Toknova, A. Kirilenko, R. Lapshin, E. Kozlov, and D. Tetyukhin, "Synthesis of biocompatible surfaces by nanotechnology methods," *Nanotechnologies in Russia*, vol. 5, no. 9-10, pp. 696–708, 2010.
- [83] S. Bertazzo and K. Rezwan, "Control of  $\alpha$ -alumina surface charge with carboxylic acids," *Langmuir*, vol. 26, no. 5, pp. 3364–3371, 2009.

- [84] G. London, K.-Y. Chen, G. T. Carroll, and B. L. Feringa, “Towards dynamic control of wettability by using functionalized altitudinal molecular motors on solid surfaces,” *Chemistry—A European Journal*, vol. 19, no. 32, pp. 10690–10697, 2013.
- [85] P. M. Ajayan and O. Z. Zhou, “Applications of carbon nanotubes,” in *Carbon nanotubes*, pp. 391–425, Springer, 2001.
- [86] M. Endo, M. S. Strano, and P. M. Ajayan, “Potential applications of carbon nanotubes,” in *Carbon nanotubes*, pp. 13–62, Springer, 2007.
- [87] R. E. Smalley, M. S. Dresselhaus, G. Dresselhaus, and P. Avouris, *Carbon nanotubes: synthesis, structure, properties, and applications*, vol. 80. Springer Science & Business Media, 2003.
- [88] L. Girifalco, M. Hodak, and R. S. Lee, “Carbon nanotubes, buckyballs, ropes, and a universal graphitic potential,” *Physical Review B*, vol. 62, no. 19, p. 13104, 2000.
- [89] K. S. Coleman, S. R. Bailey, S. Fogden, and M. L. Green, “Functionalization of single-walled carbon nanotubes via the bingel reaction,” *Journal of the American Chemical Society*, vol. 125, no. 29, pp. 8722–8723, 2003.
- [90] F. Liang, A. K. Sadana, A. Peera, J. Chattopadhyay, Z. Gu, R. H. Hauge, and W. Billups, “A convenient route to functionalized carbon nanotubes,” *Nano Letters*, vol. 4, no. 7, pp. 1257–1260, 2004.
- [91] J. Chen, H. Liu, W. A. Weimer, M. D. Halls, D. H. Waldeck, and G. C. Walker, “Noncovalent engineering of carbon nanotube surfaces by rigid, functional conjugated polymers,” *Journal of the American Chemical Society*, vol. 124, no. 31, pp. 9034–9035, 2002.
- [92] Wikipedia, “Plasma ashing — wikipedia, the free encyclopedia,” 2016. [Online; accessed 22-September-2016].
- [93] K. Inomata, H. Koinuma, Y. Oikawa, and T. Shiraishi, “Open air photore-sist ashing by a cold plasma torch: Catalytic effect of cathode material,” *Applied physics letters*, vol. 66, no. 17, pp. 2188–2190, 1995.

- [94] J. Chung, M. Jeng, J. Moon, A. Wu, T. Chan, P. Ko, and C. Hu, “Deep-submicrometer mos device fabrication using a photoresist-ashing technique,” *IEEE electron device letters*, vol. 9, no. 4, pp. 186–188, 1988.
- [95] H. Song, P. Xiao, X. Qiu, and W. Zhu, “Design and preparation of highly active carbon nanotube-supported sulfated tio 2 and platinum catalysts for methanol electrooxidation,” *Journal of Power Sources*, vol. 195, no. 6, pp. 1610–1614, 2010.
- [96] J.-L. Salager, “Surfactants types and uses,” *Fire p booklet-E300-attaching aid in surfactant science and engineering in English. Merida Venezuela*, vol. 2, p. 3, 2002.
- [97] M. Reiners, K. Xu, N. Aslam, A. Devi, R. Waser, and S. Hoffmann-Eifert, “Growth and crystallization of tio2 thin films by atomic layer deposition using a novel amido guanidinate titanium source and tetrakis-dimethylamido-titanium,” *Chemistry of Materials*, vol. 25, no. 15, pp. 2934–2943, 2013.
- [98] K. Esumi, M. Ishigami, A. Nakajima, K. Sawada, and H. Honda, “Chemical treatment of carbon nanotubes,” *Carbon*, vol. 34, no. 2, pp. 279–281, 1996.
- [99] S. W. Lee, B.-S. Kim, S. Chen, Y. Shao-Horn, and P. T. Hammond, “Layer-by-layer assembly of all carbon nanotube ultrathin films for electrochemical applications,” *Journal of the American Chemical Society*, vol. 131, no. 2, pp. 671–679, 2008.
- [100] H. R. Byon, J. Suntivich, E. J. Crumlin, and Y. Shao-Horn, “Fe-n-modified multi-walled carbon nanotubes for oxygen reduction reaction in acid,” *Physical Chemistry Chemical Physics*, vol. 13, no. 48, pp. 21437–21445, 2011.
- [101] J.-B. Park, J. Hassoun, H.-G. Jung, H.-S. Kim, C. S. Yoon, I.-H. Oh, B. Scrosati, and Y.-K. Sun, “Influence of temperature on lithium–oxygen battery behavior,” *Nano letters*, vol. 13, no. 6, pp. 2971–2975, 2013.
- [102] P. Tan, W. Shyy, T. Zhao, Z. Wei, and L. An, “Discharge product morphology versus operating temperature in non-aqueous lithium-air batteries,” *Journal of Power Sources*, vol. 278, pp. 133–140, 2015.

- [103] J. Adams, M. Karulkar, and V. Anandan, "Evaluation and electrochemical analyses of cathodes for lithium-air batteries," *Journal of Power Sources*, vol. 239, pp. 132–143, 2013.
- [104] A. Débart, A. J. Paterson, J. Bao, and P. G. Bruce, " $\alpha$ -mno<sub>2</sub> nanowires: A catalyst for the o<sub>2</sub> electrode in rechargeable lithium batteries," *Angewandte Chemie*, vol. 120, no. 24, pp. 4597–4600, 2008.
- [105] H. Cheng and K. Scott, "Carbon-supported manganese oxide nanocatalysts for rechargeable lithium–air batteries," *Journal of Power Sources*, vol. 195, no. 5, pp. 1370–1374, 2010.
- [106] S. Meini, M. Piana, H. Beyer, J. Schwämmlein, and H. A. Gasteiger, "Effect of carbon surface area on first discharge capacity of li-o<sub>2</sub> cathodes and cycle-life behavior in ether-based electrolytes," *Journal of The Electrochemical Society*, vol. 159, no. 12, pp. A2135–A2142, 2012.
- [107] N. G. Akalework, C.-J. Pan, W.-N. Su, J. Rick, M.-C. Tsai, J.-F. Lee, J.-M. Lin, L.-D. Tsai, and B.-J. Hwang, "Ultrathin tio<sub>2</sub>-coated mwcnts with excellent conductivity and smsi nature as pt catalyst support for oxygen reduction reaction in pemfcs," *Journal of Materials Chemistry*, vol. 22, no. 39, pp. 20977–20985, 2012.
- [108] T. Okpalugo, P. Papakonstantinou, H. Murphy, J. McLaughlin, and N. Brown, "High resolution xps characterization of chemical functionalised mwcnts and swcnts," *Carbon*, vol. 43, no. 1, pp. 153–161, 2005.
- [109] W. Xu, J. Hu, M. H. Engelhard, S. A. Towne, J. S. Hardy, J. Xiao, J. Feng, M. Y. Hu, J. Zhang, F. Ding, *et al.*, "The stability of organic solvents and carbon electrode in nonaqueous li-o<sub>2</sub> batteries," *Journal of Power Sources*, vol. 215, pp. 240–247, 2012.